UNIVERSITÀ
DEGLI STUDI
DI PADOVA

Sede amministrativa: Università degli Studi di Padova

Dipartimento di Biologia

SCUOLA DI DOTTORATO DI RICERCA IN BIOSCIENZE E BIOTECNOLOGIE

INDIRIZZO DI NEUROBIOLOGIA

CICLO 27°

ROLE OF MITOCHONDRIAL Ca^{2+} UPTAKE IN BREAST CANCER CELL MIGRATION AND INVASIVENESS

Direttore della Scuola: Ch.mo Prof. Giuseppe Zanotti

Coordinatore d'indirizzo: Ch.ma Prof. Daniela Pietrobon

Supervisore: Ch.mo Prof. Rosario Rizzuto

Dottoranda: Anna Tosatto

TABLE OF CONTENTS

SUMMARY

Mitochondrial Ca^{2+} uptake regulates cellular energetic by triggering ATP synthesis. At the same time, Ca^{2+}_{mit} acts as key controller of both cell metabolism and fate. Indeed, a decrease in ATP production elicits autophagy induction, while Ca^{2+} overload causes organelle dysfunction and release of caspase cofactors (Glancy and Balaban, 2012; Jouaville et al., 1999; Rizzuto et al., 2012).

Several pathological conditions, including tumor formation and progression, are directly related to mitochondrial dysfunctions, and reprogramming of mitochondrial metabolism is now considered as an emerging hallmark of cancer. Indeed, even in the presence of oxygen, cancer cells limit their energy supply largely to glycolysis, leading to the so called “aerobic glycolysis” phenotype (Gaude and Frezza, 2014; Hanahan and Weinberg, 2011; Sciacovelli et al., 2014). Of note, the dependence on glycolytic fueling is further potentiated by hypoxia, a condition that characterizes most tumor microenvironments. Indeed, in response to oxygen deprivation, the hypoxia-indicible-factor-1α (HIF-1α) is stabilized and, consequently, transcription of glucose transporters and glycolysis-related enzymes is induced (Semenza, 2010a, b). In addition, several hereditary tumors have been associated with mutations in key mitochondrial enzymes showing that, in specific settings, an altered mitochondrial metabolism represents a primary trigger for cancer progression (Gottlieb and Tomlinson, 2005).

Consistent with these observations, among the most aggressive human breast tumors, triple-negative-breast-cancers (TNBC), a clinically heterogeneous category of breast tumors that lack expression of estrogen, progesterone and HER2 receptors, show profound metabolic alterations with impaired mitochondrial oxidative metabolism (Elias, 2010; Owens et al., 2011).

Our preliminary observations suggested that, in contrast to pre-malignant cells, TNBC metastatic cells accumulate high [Ca^{2+}] into the mitochondrial matrix upon agonist stimulation. These elevate Ca^{2+}_{mit} transients might be essential for metastatic progression, while sensitize premalignant cells to apoptotic stimuli. Accordingly, we hypothesized alternative roles of mitochondrial Ca^{2+}, distinct from mitochondrial energy production and control of cell death, possibly involved in the metastatic progression of these highly malignant breast tumors.

The molecular characterization of the Mitochondrial Calcium Uniporter (MCU), the highly selective channel responsible for Ca^{2+}_{mit} entry into the matrix, opened the chance to modulate mitochondrial function by modifying MCU channel's activity.

We demonstrated that both pharmacological and genetic inhibition of MCU causes a significant decline in TNBC metastatic cell motility and invasiveness.

Thus, we investigated how Ca^{2+}_{mit} uptake contributes to mitochondrial Reactive-Oxygen-Species (mROS) production, thus playing a crucial role in the regulation of ROS-dependent cascades. Indeed, ROS molecules are considered fundamental molecular effectors for cancer progression, by eliciting metabolic adaptations and *in vivo* metastasis formation (Porporato et al., 2014; Tochhawng et al., 2013). Coherently, we observed that antioxidant treatments reduce significantly MDA-MB-231 cell migration. Moreover, in the absence of MCU, production of mROS is significantly reduced, suggesting that mROS might play a crucial role in cell malignancy regulation by Ca^{2+}_{mit} uptake. In addition, MCU silencing inhibits hypoxia-inducible factor 1α (HIF-1α) transcription, thus impairing the expression of HIF-target genes involved in metastasis progression, possibly in a ROS-dependent manner. Of note, rescue of HIF-1α expression restores migration of MCU-silenced TNBC cells.

Our results highlight a crucial role of MCU in the control of TNBC metastatic potential and indicate that mitochondrial Ca^{2+} uptake could represent a novel therapeutic target for clinical intervention.

RIASSUNTO (ITALIANO)

Il flusso di Ca^{2+} mitocondriale (Ca^{2+}_{mit}) è il principale regolatore della bioenergetica cellulare, grazie al fatto che stimola la produzione di ATP. Allo stesso tempo, il Ca^{2+}_{mit} gioca un ruolo chiave nella regolazione sia del metabolismo sia della morte cellulare. Infatti, una diminuita produzione di ATP porta all'attivazione del processo autofagico (per compensare la mancanza di nutrienti) mentre un accumulo elevato di Ca^{2+} nel mitocondrio porta inevitabilmente ad una disfunzione dell'organello, seguita dall'attivazione caspasica e quindi dalla morte cellulare (Glancy and Balaban, 2012; Jouaville et al., 1999; Rizzuto et al., 2012). Molte patologie, tra cui la formazione e crescita tumorale, sono direttamente correlabili con le disfunzioni mitocondriali. Inoltre, il reprogramming del metabolismo mitocondriale è ora considerato un aspetto chiave nella patogenesi del cancro. Infatti, anche in presenza di ossigeno, le cellule tumorali limitano gran parte del loro supporto energetico alla glicolisi, raggiungendo lo stato energetico denominato "glicolisi aerobica" (Gaude and Frezza, 2014; Hanahan and Weinberg, 2011; Sciacovelli et al., 2014). Vale la pena evidenziare che la dipendenza energetica da un regime glicolitico può venir ulteriormente rafforzata in ipossia, condizione che contraddistingue la maggior parte dei microambienti tumorali. Infatti, in risposta alla carenza di ossigeno, il fattore trascrizionale HIF-1α viene stabilizzato e, di conseguenza, viene indotta la trascrizione di proteine di trasporto del glucosio e di enzimi coinvolti direttamente nel metabolismo glicolitico (Semenza, 2010a, b). Inoltre, molti tumori ereditari sono stati associati a mutazioni a carico di enzimi mitocondriali, dimostrando in questo modo che, in particolari condizioni, un'alterazione del metabolismo mitocondriale può esser considerata fattore eziologico per lo sviluppo del tumore (Gottlieb and Tomlinson, 2005).

A supporto di queste considerazioni, il tumore mammario metastatico triplo negativo, una delle più aggressive ed eterogenee classi di tumori caratterizzata dalla mancata espressione dei recettori estrogenici, progestinici ed HER2, mostra una profonda alterazione metabolica con ridotta attività ossidativa mitocondriale (Elias, 2010; Owens et al., 2011).

I nostri risultati preliminari suggeriscono che, al contrario delle cellule pre-maligne, le metastatiche triplo negative riescono ad accumulare, dopo stimolazione, alte [Ca^{2+}] all'interno della matrice mitocondriale. Transienti di Ca^{2+}_{mit} così elevati possono risultare addirittura essenziali per la progressione metastatica, mentre in cellule pre-maligne sensibilizzano alla morte cellulare. Di conseguenza, abbiamo ipotizzato ruoli alternativi per il Ca^{2+}_{mit}, possibilmente coinvolti nello sviluppo metastatico, che fossero diversi da quelli di produzione energetica mitocondriale e di controllo dell'apoptosi.

La caratterizzazione molecolare dell'Uniporto Mitocondriale del Calcio (dall'inglese MCU), canale selettivo per il Ca^{2+} che ne regola l'ingresso all'interno della matrice, ha aperto la possibilità di modulare la funzione mitocondriale modificando l'attività del canale MCU.

Così, si è deciso di investigare come l'ingresso di Ca^{2+}_{mit} contribuisca alla produzione mitocondriale di specie radicaliche dell'ossigeno (ROS), giocando in questo modo un ruolo cruciale nella regolazione di tutti i meccanismi di segnale ROS-dipendenti: i ROS sono considerati dei critici effettori molecolari della progressione tumorale, promuovendo l'adattamento metabolico e la formazione di metastasi *in vivo* (Porporato et al., 2014; Tochhawng et al., 2013). Di conseguenza, si è osservato che trattamenti antiossidanti riducono significativamente la migrazione delle cellule tumorali triple negative MDA-MB-231. Inoltre, è stato verificato che, in assenza di MCU, la produzione di ROS è significativamente ridotta, suggerendo così che i ROS mitocondriali giocano un ruolo cruciale nella regolazione della malignità tumorale mediata dal Ca^{2+}_{mit}. In aggiunta, è stato dimostrato che il silenziamento di MCU inibisce significativamente la trascrizione del fattore

di trascrizione HIF-1α, riducendo di conseguenza l'espressione dei geni da lui regolati, soprattutto di quelli coinvolti nella progressione metastatica e possibilmente con un meccanismo ROS-dipendente. Da notare, a tal proposito, che la ri-espressione di HIF-1α ripristina completamente la capacità di migrazione nelle cellule in cui MCU è silenziato.

In conclusione, i nostri risultati mettono in luce un ruolo cruciale di MCU nel controllo del potenziale metastatico del tumore mammario triplo negativo ed indicano che il flusso mitocondriale di Ca^{2+} può rappresentare un nuovo bersaglio terapeutico per un innovativo approccio clinico.

INTRODUCTION

CANCER BIOLOGY

Metabolic reprogramming: a hallmark of cancer.

Cancer is a heterogeneous disease, both biologically and clinically, with distinct histological and genetic features. Nevertheless, all tumors are characterized by some biological hallmarks among which unrestrained proliferation is the most represented (Hanahan and Weinberg, 2011). Several findings indicate that cancer cells undergo a complex metabolic reprogramming to satisfy the increased requirement of macromolecules and energy necessary for proliferation. The hypothesis that cancer cell metabolism is altered dates back to several decades ago. Actually, it was at the beginning of the twentieth century, thanks to the emerging biochemistry discoveries, that the energy requirements of cell proliferation were initially taken into consideration. The German scientist von Wassermann, an illustrious bacteriologist, was the first who hypothesized that cancer cells increase oxygen consumption to satisfy their accelerated proliferation rate. Consistent with this hypothesis, he started targeting cancer cells using a derivative compound of selenium (selenium–eosin), a drug that was thought to disrupt cell respiration (Wassermann, Keysser, & Wassermann, 1911). Despite very promising trials in rodents, this drug was found to be highly toxic in humans, and further investigations revealed that selenium was not as useful in killing cancer cells as initially thought, making Wassermann's observations fruitless (Sugiura & Benedict, 1929). A more systematic study of cancer metabolism started some years later, thanks to the meticulous effort of Otto Warburg. In his early career, he observed that cancer cells consume large amounts of glucose through glycolysis even in the presence of oxygen, whereas normal cells predominantly use respiration as main energy source (Warburg et al., 1927). He further hypothesized that cancer transformation was caused by inherent defects in mitochondrial function (Warburg, 1956). Despite debated, Warburg's observations

prompted to understand the biochemical determinants of cancer transformation (Weinhouse, 1976). Afterwards, the elucidation of the DNA structure and the discovery of oncogenes and tumor-suppressors in cancer, in the late 1970s, temporarily diverted the scientific interest to the emerging cancer genetics field.

Cancer metabolism had been partially neglected until the late 1990s, when the laboratory of Chi Van Dang demonstrated that c-Myc oncogene actively contributes to aerobic glycolysis by controlling the expression of the glycolytic enzyme lactate dehydrogenase-A (Shim et al., 1997), revamping the field of cancer metabolism. At this stage, however, altered metabolism was seen as nothing more than an epiphenomenon of cell transformation, a by-product of the oncogene-induced reprogramming. The link between metabolism and cancer progression was further corroborated in the early 2000s, by the discovery that mutations of housekeeping metabolic enzymes such as succinate dehydrogenase (SDH) (Baysal et al., 2000) and fumarate hydratase (FH) (Tomlinson et al., 2002) were associated with hereditary forms of cancer. This finding highlighted the possibility that, under some circumstances, altered metabolism could be the cause, not the consequence, of cancer transformation (Gottlieb and Tomlinson, 2005).

These observations inspired a renewal of the cancer metabolism field, which combined biochemical knowledge on cell metabolism developed in the pre-genomic era, with novel high-throughput techniques such as transcriptomics and metabolomics. These multidisciplinary efforts culminated with the discovery that a huge number of oncogenes and tumor suppressors are implicated in the regulation of cancer cell metabolism (e.g. Ras and Akt mutations increase glycolytic flux at different levels (Hsu and Sabatini, 2008)) and that key metabolic enzymes, if mutated, predispose to cancer. It is now clear that metabolic reprogramming is an obligate step of cancer transformation, required to sustain unrestrained proliferation triggered by the activation of oncogenic signalling cascades, which

turns tumor metabolism from an anecdotal evidence to a hallmark of cancer (Hanahan and Weinberg, 2011).In this chapter, we will discuss aerobic glycolysis, the major component of cancer cells metabolic transformation, and how it contributes to cancer growth and proliferation.

Aerobic glycolysis

Non-proliferating cells of differentiated tissues predominantly use mitochondrial oxidative phosphorylation (OXPHOS) to fuel their energetic needs. In sharp contrast, in tissue with high proliferative rate, as well as in cancer, metabolic pathways shift toward an anabolic metabolism, endowed with a high glucose utilization, lactate production and biosynthesis of macromolecules (Fig. 1) (Fritz and Fajas, 2010).

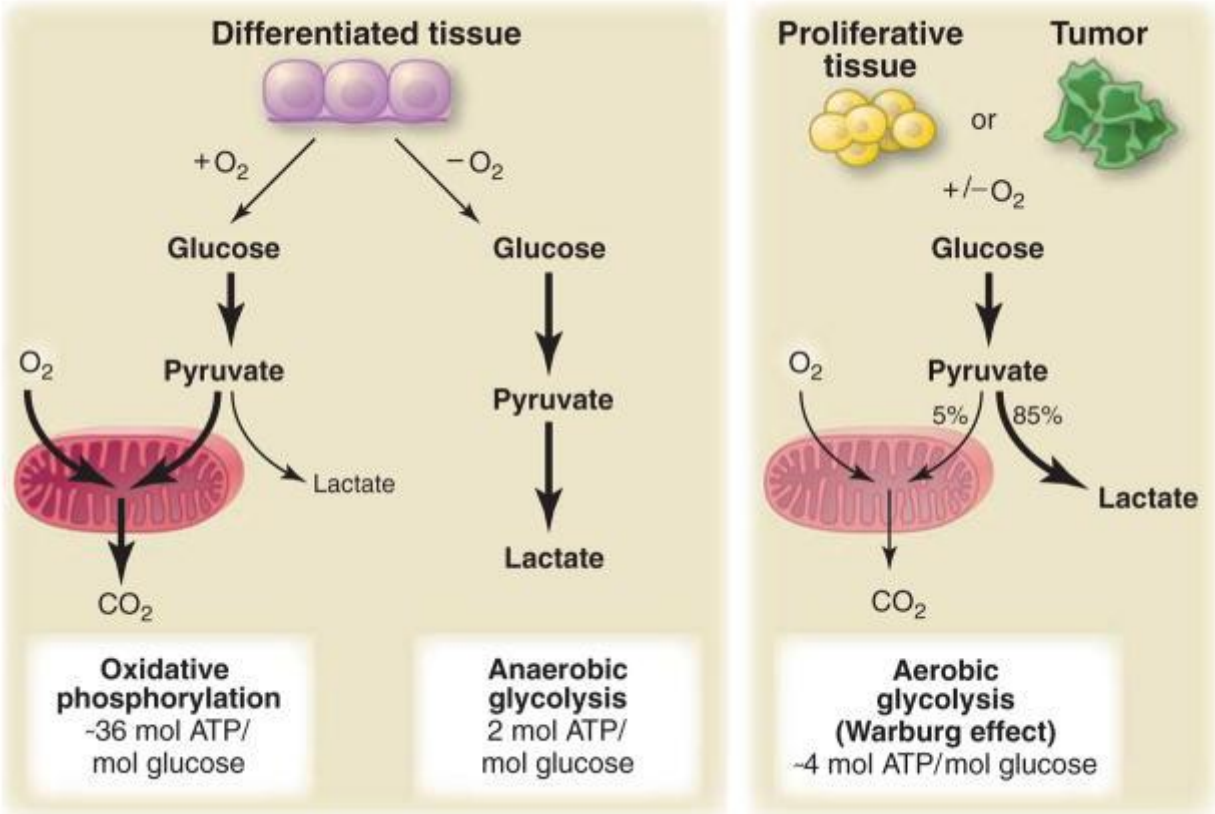

FIG.1. Schematic differences between oxidative phosphorylation, anaerobic glycolysis and aerobic glycolysis (Vander Heiden et al., 2009)

Aerobic glycolysis is the metabolic process that converts glucose into lactate even under aerobic conditions, when normal cells fully oxidize glucose in the mitochondria. Today, induction of aerobic glycolysis in tumor cells is called the "Warburg effect" and was initially thought to be caused by inherent mitochondrial dysfunction (Warburg, 1956). However, the oxidative capacity of mitochondria in cancer cells is intact. We now know that aerobic glycolysis is genetically determined (Levine and Puzio-Kuter, 2010) and its role in supporting proliferation goes beyond cancer cells. Indeed, aerobic glycolysis has been observed also in non-transformed cells, including activated lymphocytes (Wang and Green, 2012) and embryonic stem cells (Zhang et al., 2012). These observations indicate that aerobic glycolysis can be considered a common metabolic phenotype (metabotype) of proliferating cells. However, the reasons why cancer cells switch to aerobic glycolysis are still debated.

Glycolysis, the process that converts glucose into pyruvate, generates 2 molecules of ATP per molecule of glucose, whereas the full oxidation of glucose through mitochondria generates 31 molecules of ATP. Based on pure stoichiometric calculations, aerobic glycolysis should be an inefficient pathway for ATP generation, and the switch to this metabotype seems a paradox for cancer cells. However, the current model postulates that the preferential use of aerobic glycolysis offers the following advantages to highly proliferative cells.

First, it focuses cells on the use of glucose, which is the most abundant extracellular nutrient. Second, glycolysis is not inefficient at providing cells with ATP, if considering kinetic aspects. Actually, although glycolysis generates ATP with lower efficiency than oxidative phosphorylation, it produces ATP at a faster rate, when glucose is provided at a sufficiently high concentration (Pfeiffer et al., 2001). Furthermore, the glycolytic flux is so efficient in

cancer cells compared to non-transformed cells that, by the time one molecule of glucose is fully oxidized via respiration, 24 additional ATPs are generated via aerobic glycolysis, demonstrating that aerobic glycolysis could still supply 2/3 of the ATP, if respiration fails (Koppenol et al., 2011).

Third, glucose utilization provides essential metabolic intermediates for the biosynthesis of diverse macromolecules such as lipids, nucleic acids, non-essential amino acids cysteine, glycine, serine and alanine, and for anti-oxidative defenses (Kondoh et al., 2007; Vander Heiden et al., 2009).

Given the large amount of glucose taken up by cancer cells in the unit time, it has been speculated that the amount of ATP generated by aerobic glycolysis might even exceed the ATP requirements of cancer cells. Importantly, without sufficient ATP turnover, ADP and phosphate would become a limiting factor for glycolysis, and the accumulation of ATP would cause the allosteric inhibition of key metabolic enzymes, such as phosphofructokinase (PFK1), blocking the entire glycolytic flux. Therefore, it has been proposed that aerobic glycolysis must be coupled to, or even driven by, aberrant ATP-consuming reactions present in cancer cells (Racker, 1976).

A defective Na+/K+ plasma membrane ATPase has been initially proposed to be the major sink of ATP in cancer cells (Fagan and Racker, 1978). More recently, other examples of cancer-specific ATP-consuming reactions have been reported. The first case entails the upregulation of the ER-enzyme ENTPD5, which engages into an ATP-hydrolyzing futile cycle resulting in a compensatory increase in aerobic glycolysis (Fang et al., 2010). The second example involves the expression of the cancer-specific M2 variant of pyruvate kinase (PKM2), which was shown to uncouple pyruvate production from ATP generation, by stimulating the transfer of the high-energy phosphate of phosphoenolpyruvate to the

glycolytic enzyme phosphoglycerate-mutase (PGAM), instead of ADP (Vander Heiden et al., 2010). The molecular mechanisms responsible for aerobic glycolysis shift still remain an exciting scientific challenge.

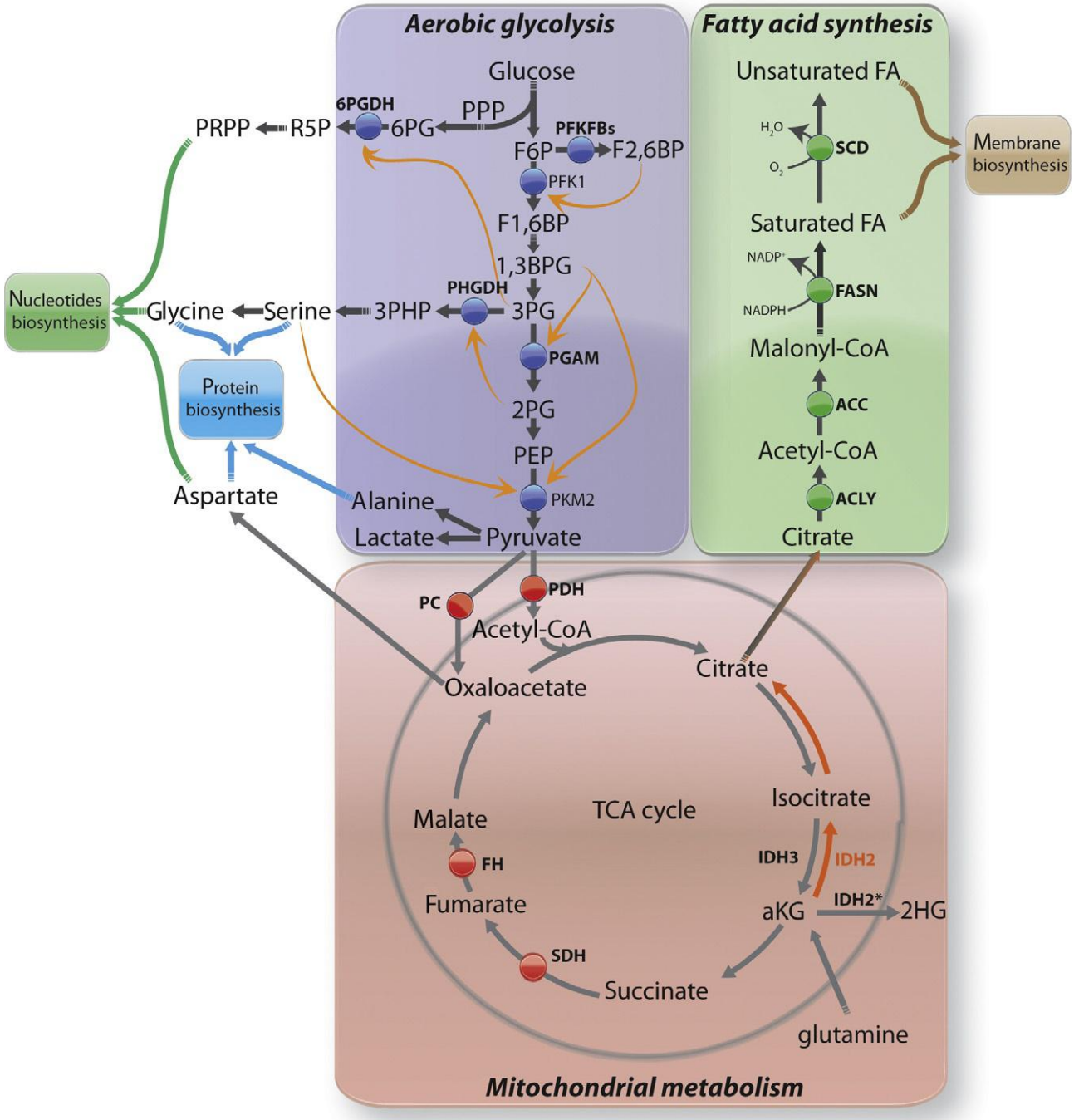

FIG.2. Three major components of the metabolic transformation of cancer cells are depicted: aerobic glycolysis, mitochondrial metabolism, and lipid synthesis (Sciacovelli et al., 2014).

Hypoxia in malignant progression

Clinical investigations carried out over the last two decades have clearly demonstrated that the prevalence of hypoxic tissue areas [i.e., areas with O_2 tensions (pO2 values) ≤2.5 mmHg] is a characteristic pathophysiological property of locally advanced solid tumors (Vaupel et al., 2004). Up to 50–60% of locally advanced solid tumors may exhibit hypoxic and/or anoxic tissue areas that are heterogeneously distributed within the tumor mass. Hypoxic/ anoxic areas arise as a result of an imbalance between supply and consumption of oxygen. Whereas in normal tissues or organs O_2 supply matches the metabolic requirements, in solid tumors, the O_2 consumption rate may exceed the limited O_2 supply and result in the development of tissue areas with very low [O_2]. Cells exposed to hypoxia respond by reducing their overall protein synthesis which in turn leads to restrained proliferation and cell cycle reprogramming. Hypoxia can hinder or even completely inhibit tumor cell proliferation in vitro; the degree of inhibition depends on the severity and duration of hypoxia. Additionally, hypoxia can induce programmed cell death (apoptosis) both in normal and in neoplastic cells (Vaupel and Harrison, 2004; Vaupel and Mayer, 2007).

However, sustained hypoxia may also result in a more malignant progression characterized by a clinically aggressive phenotype. Depending on the level and (possibly) the duration of hypoxia, three processes may be involved in hypoxia-induced tumor progression: alterations in gene expression with subsequent changes of the proteome, changes in the genome, and clonal selection (Harris, 2002; Semenza, 2000, 2002). Hypoxia-induced proteome and/or genome changes leading to cell cycle arrest, differentiation, apoptosis, and necrosis, may explain delayed recurrences, dormant micrometastases, and growth retardation which can occur in large tumors. This proteome changes promote tumor progression via mechanisms enabling cells to overcome nutritive deprivation, to escape from the hostile environment and to favor unrestricted growth; tumor quiescent cells that survived under hypoxic

conditions may develop an increased potential for local invasive growth and distant metastasis, resulting in a poor prognosis (Vaupel and Mayer, 2007).

A major mechanism mediating these adaptive responses to reduced O_2 availability is the regulation of transcription by hypoxia-inducible-factor-1 (HIF-1) (Semenza, 2010b). HIF-1 is a heterodimeric protein composed of a constitutively expressed HIF-1β subunit and an O_2-regulated HIF-1α subunit. HIF-1α is subjected to O_2-dependent hydroxylation on proline residues 402 and 564 by prolyl-hydroxylase-domain-protein-2 (PHD2) and this modification creates an interface for interaction with the von Hippel–Lindau tumor suppressor protein (VHL), which recruits an E3 ubiquitin-protein ligase that catalyzes polyubiquitination of HIF-1α, thereby targeting it for proteasomal degradation.

Under hypoxic conditions, hydroxylation is inhibited, thus HIF-1α rapidly accumulates, dimerizes with HIF-1β, and activates transcription of target genes. O_2-dependent hydroxylation of asparagine-803 by factor inhibiting HIF-1 (FIH-1) impairs the interaction of HIF-1α with the transcription co-activators P300 and CBP under normoxic conditions. Both PHD2 and FIH-1 use O_2 and α-ketoglutarate as substrates and generate CO_2 and succinate as by-products of the hydroxylation reaction.

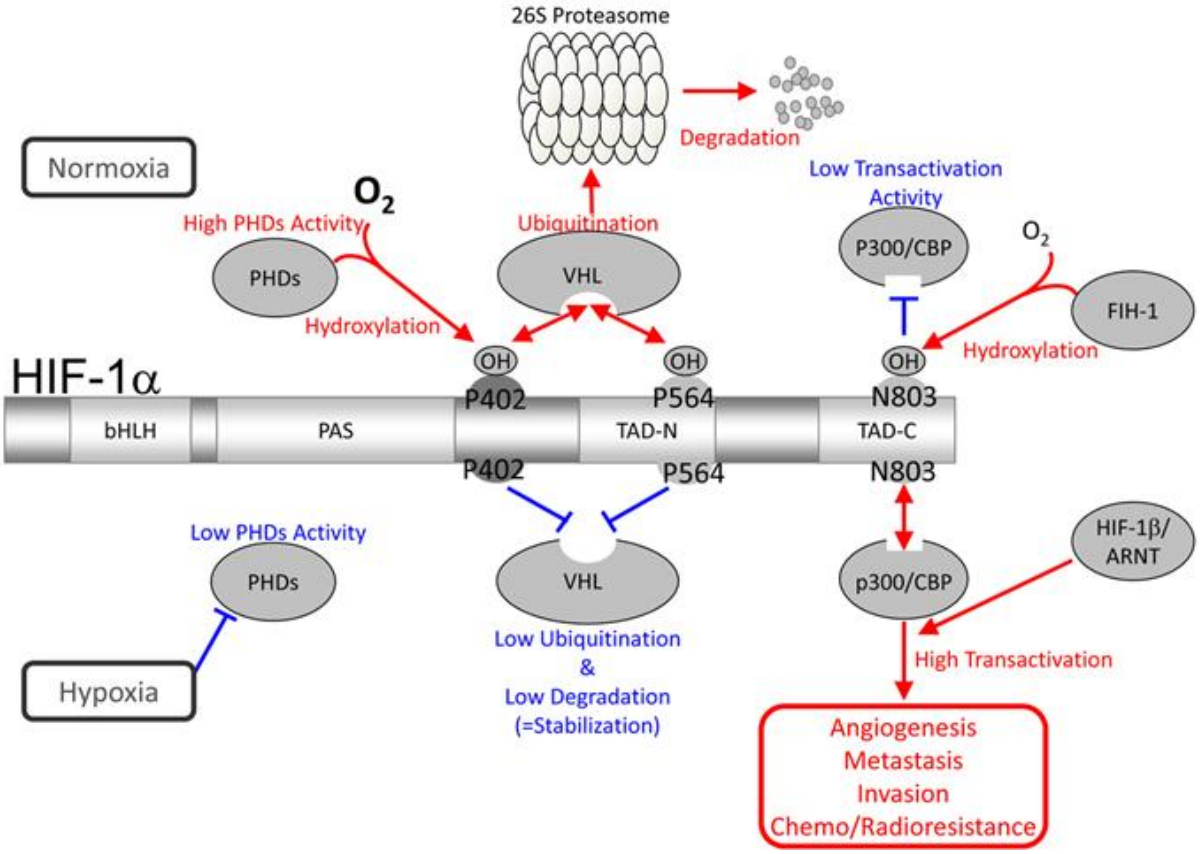

FIG.3. Molecular mechanism underlying the activation of HIF-1 under hypoxic conditions (Harada H., Gene Therapy Strategy for Tumour Hypoxia, 2011).

HIF-2α is a protein with high sequence similarity to HIF-1α. Similarly to HIF-1α, HIF-2α is regulated by proline and asparagine hydroxylation, dimerizes with HIF-1β and activates transcription of a group of target genes that overlaps with, but is distinct from, those regulated by HIF-1α.

HIF-3α is an inhibitor of HIF-1α that may be involved in feedback regulation as suggested by the fact that its expression is transcriptionally regulated by HIF-1α.

Immunohistochemical analysis of biopsies revealed increased levels of HIF-1α or HIF-2α protein (or both) in the majority of primary human cancers and their metastases (compared to surrounding normal tissue).

HIF-1α can be regulated even under normoxic conditions by a number of oncogenes (i.e. Ras, SRC and PI3K) or loss of tumor suppressors such as VHL (von Hippel–Lindau) or PTEN phosphatase. Furthermore, increased levels of metabolites i.e. succinate and fumarate (King et al.2006), or O_2 byproducts like free radicals, can also stabilize HIF-1α (Quintero et al., 2006).

The variety of genes that are induced by hypoxia in an HIF-1-dependent manner encode proteins that have key roles in every critical aspect of cancer biology (Fig.4), including angiogenesis, cell survival, chemotherapy and radiation resistance, immortalization, immune evasion, invasion and metastasis, proliferation, glucose metabolism and pH regulation, and stem cell maintenance.

HIF-1α stimulates glycolysis by inducing the expression of glucose transporters GLUTs, which are responsible for glucose uptake, and of several enzymes of the glycolytic chain (for example hexokinase, phosphofructokinase 1 and aldolase); second, HIF-1α downregulates oxidative phosphorylation, by inducing the expression of pyruvate dehydrogenase kinase 1 (PDK1), which inhibits the entry of pyruvate into the Krebs cycle by phosphorylation of pyruvate dehydrogenase.

Gene product	*Role in cancer progression*
Angiopoietin 2	Angiogenesis, lymphangiogenesis
Angiopoietin-like 4	Metastasis
Breast cancer resistance protein (ABCG2)	Multidrug transport, stem cell maintenance
Carbonic anhydrase 9 and 12	pH regulation
C-MET	Invasion
CXCR4	Metastasis
DEC1	Genomic instability
Endothelin 1	Invasion
Fibronectin 1	Invasion
Glucose phosphate isomerase	Cell motility, glucose metabolism, immortalization
Glucose transporter 1	Glucose uptake
Hexokinase 1 and 2	Glucose phosphorylation, cell survival
Inhibitor of differentiation 2	Angiogenesis, proliferation
Insulin-like growth factor 2	Cell survival, proliferation
JARID1B	Stem cell maintenance
Kit ligand (stem cell factor)	Angiogenesis, stem cell maintenance
Lactate dehydrogenase A	Glucose metabolism
Lysyl oxidase	Metastasis
Matrix metalloproteinase 2 and 14	Invasion
NT5E (ecto-5′-nucleotidase/CD73)	Immune evasion, multidrug resistance
OCT4	Stem cell maintenance
Placental growth factor	Angiogenesis
Platelet-derived growth factor B	Cell proliferation/survival, angiogenesis
Pyruvate dehydrogenase kinase 1	Glucose metabolism
Pyruvate kinase M2	Glucose metabolism
Stromal-derived factor 1	Angiogenesis
Survivin	Cell survival
Telomerase	Immortalization
Transforming growth factor-α	Cell proliferation/survival
TWIST1	Epithelial–mesenchymal transition
Urokinase plasminogen activator receptor	Invasion
Vascular endothelial growth factor	Angiogenesis
WSB1	Cell survival
ZEB1 (ZFHX1A), *ZEB2* (ZFHX1B)	Epithelial–mesenchymal transition

FIG.4. Selected HIF-1 target genes whose products contribute to cancer progression (Semenza, 2009).

REACTIVE OXYGEN SPECIES

ROS molecules

Oxygen is an indispensable molecule for the aerobic organisms. However, Reactive Oxygen Species (ROS), which are generated by partial O_2 reduction, can be formed by a variety of mechanisms, including generation during oxidative phosphorylation in the mitochondria, as a byproduct of normal cellular aerobic metabolism (Davies, 1995). Indeed, in the aerobic environment, mitochondrial ATP generation is coupled to the reduction of molecular oxygen to water and to electron transport in the respiratory chain. Reactive oxygen species (ROS) are principally formed by complex I and III. Indeed, free electrons responsible for ROS generation are released by oxidation of high energy molecules, such as NADH and FAD, and carried by "electron carriers" such as Coenzyme Q and Cytochrome C.

In details, molecular oxygen is found in nature as a diatomic molecule, presenting two unpaired electrons with parallel spin in its outermost shell (triplet oxygen) and this configuration makes it non reactive and weak oxidant. The complete reduction of one molecule of oxygen to 2 molecules of water, at complex IV, requires the transfer of 4 electrons. However, during electron transfer, some electrons leak out and react with environmental O_2, leading to an incomplete reduction of molecular O_2, thus producing reactive intermediates. The products of partial oxygen reduction are the following:

- Singlet oxygen ($^1O_2$): singlet oxygen is commonly formed following exposure to UV or visible light in the presence of chromophores that can act as sensitising agents. However, it can also be formed by a range of peroxidase enzymes or during the reaction of H_2O_2 with peroxynitrite. $^1O_2$ interacts with a wide range of biological targets, including DNA, RNA, proteins, lipids and sterols (Davies, 2003).
- Superoxide anion (O_2^-): the biological toxicity of superoxide is due to its capacity to inactivate iron-sulfur cluster containing enzymes, critical in a wide variety of metabolic

pathways, thereby liberating free iron in the cell, which can generate the highly reactive hydroxyl radical. In its HO2 form (hydroperoxyl radical) superoxide can also initiate lipid peroxidation. Superoxide can also react with nitric oxide (NO) to form ONOO-. As such, superoxide is one of the main causes of oxidative stress. Superoxide can also produce hydrogen peroxide through a dismutation reaction catalyzed by superoxide dismutase.

- Hydrogen peroxide (H2O2): it is formed by superoxide anion dismutation. It is lipid soluble and thus able to diffuse across membranes. Depending on concentrations, H2O2 can act as a signaling molecule. However, it can be a dangerous species for the biological systems, as in the presence of ions, such as Fe2+ e Cu+, it can generate highly reactive hydroxyl radical.
- Hydroxyl radical ($OH^{\bullet -}$): it is the most dangerous reactive oxygen species. The hydroxyl radical cannot be eliminated by an enzymatic reaction, as this would require its diffusion to the enzyme's active site. As diffusion is slower than the half-life of the molecule, it reacts with any oxidizable compound in its vicinity. It can damage virtually all types of macromolecules: carbohydrates, nucleic acids (mutations), lipids (lipid peroxidation) and amino acids. The only means to protect important cellular structures is the use of effective repair systems and antioxidants.

ROS induced damage and anti-oxidant defence

It has been demonstrated that ROS are involved in numerous pathophysiological conditions, such as ageing, cancer, myocardial infarct, neurodegenerative diseases and many others (Droge, 2002). The effects of oxidative stress on cellular responses including signaling and transcription have been attributed to the oxidative modification of macromolecules like

proteins, nucleic acids and lipids. Different protein modification have been described that include modifications of targets via oxidation of the sulfhydryl (-SH) group of cysteine residues, conformational changes due to oxidation-induced intramolecular disulfide bridge formation and inter-molecular disulfide bridges leading to protein dimerization. Modification of critical cysteine residues of some transcription factors has also been shown to promote DNA binding and transactivation, as well as activation, of protein kinases (Thannickal and Fanburg, 2000). Because ROS react with proteins and modify their functions, ROS are likely important players in several cellular mechanisms. The initial reaction results in the formation of secondary radicals that can diffuse and lead to the propagation of the damage. These reactions can terminate only when free radicals are in the presence of molecules able to neutralize them (i.e. scavengers) or an enzymatic system, able to metabolize them.

ROS are constantly formed, even under physiological conditions. However, their production is counterbalanced by several cellular mechanisms, including enzymatic and non enzymatic pathways (Nordberg and Arner, 2001). Among the best characterized enzymatic systems are:
1. Superoxide dismutase (SOD): in eukaryotic cells, $O_2^{\bullet}$ can be metabolized to hydrogen peroxide by two metal-containing SOD isoenzymes, an 80-kDa tetrameric Mn-SOD present in mitochondria, and the cytosolic 32-kDa dimeric Cu/Zn-SOD (Weisiger and Fridovich, 1973). In the reaction catalyzed by SOD, two molecules of superoxide form hydrogen peroxide and molecular oxygen, and are thereby a source of cellular hydrogen peroxide, which is then dismutated by catalase.
2. Catalase (CAT): catalases of many organisms are mainly heme-containing enzymes. This enzyme is predominantly localized in mitochondria and peroxisomes, where it catalyzes the dismutation of hydrogen peroxide to water and molecular oxygen. One antioxidant role of catalase is to lower the risk of hydroxyl radical formation from H2O2 catalyzed by Cu+ or

Fe2+ ions. Moreover, catalase binds NADPH, which protects the enzyme from inactivation and increases its efficiency.

3. Glutathione peroxidase (GPx) and glutathione reductase (GR): there are at least four different GPx in mammals (GPx1–4), all of them containing selenocysteine (Ursini et al., 1995). GPx1 and GPx4 (or phospholipid hydroperoxide GPx) are both cytosolic enzymes abundant in most tissues. GPx is also localized at the mitochondrial level where it catalyzes the reduction of H2O2 produced by Mn-SOD, using glutathione as substrate. This system affords protection against low levels of oxidative stress, while catalase is more efficient when oxidative burden is increased. In physiological conditions, reduced glutathione (GSH) is used for the reduction of H2O2 and is transformed into oxidized glutathione (GSSH). GR is the flavoenzyme that restores GSH.

Besides the enzymatic systems, scavengers act as intracellular antioxidants: Vitamin E (N-tocopherol), Vitamin C (ascorbic acid), Glutathione (GSH), Bilirubin (the end product of heme catabolism, can efficiently scavenge peroxyl radical), Uric acid.

ROS signaling in cancer

In tumorigenic environments, increased generation of ROS often overwhelms the antioxidant systems, leading to oxidative stress. Different levels of oxidative stress appear to confer different outcomes in cancer cells: while high oxidative stress can lead to cell death (Nishikawa, 2008), mild oxidative stress at sub-lethal levels triggers activation of cell signaling mechanisms such as increased proliferation, migration and invasion (Porporato et al., 2014).

Here we will analyze the main ROS-triggered events involved in cancer progression: cell migration, cell adhesion, extra-cellular matrix invasion and epithelial-to-mesenchymal transition.

Cell migration. It is a crucial event in embryonic development, cell homeostasis, wound healing, and other pathological states such as cancer cell invasion and metastasis (Hurd et al., 2012). It encompasses a wide array of cellular changes involving alterations in cell structure by formation of protrusions required for migration and regulation of cytoskeleton dynamics, expression of adhesion molecules and activation of signaling processes necessary for cell migration.

Members of the Mitogen Activated Protein Kinase (MAPK) family, including extracellular signal-regulated kinase (ERK), the c-jun NH-2 terminal kinase (JNK), and the p-38 MAPK are activated during cell migration. One mechanism by which ROS mediate activation of these pathways is via growth factor stimulation of receptor tyrosine kinases (RTKs) (Wu et al., 2006). When generated as a result of growth factor receptor stimulation, ROS transmit signals to induce cellular changes necessary for migration. Furthermore, in endothelial cells, vascular endothelial growth factor (VEGF) has been shown to stimulate ROS production via Nox and mitochondrial-dependent pathways (Wang et al., 2011), leading to enhanced cell migration. The mechanisms of how activation of growth factor receptors stimulates ROS production remain elusive. Important signaling targets of ROS during cell migration include the protein kinase C (PKCs) as well as the protein tyrosine phosphatases (PTPs) (Wu, 2006). Both PKCs and PTPs contain critical cysteine residues that can be oxidized by ROS. PKC is activated upon oxidation while PTP is inhibited. The oxidation states of PKCs and PTPs can facilitate RTK signaling by activating the MAPK signaling cascade leading to tumor cell migration (Boivin et al., 2010; den Hertog et al., 2008). Interestingly, activated PKC in turn

can influence ROS generation, suggesting the existence of a positive feedback mechanism from ROS to PKC and vice versa, resulting in signal amplification that enhances cell migration.

Cell adhesion. The role of ROS in cell adhesion is well established, since integrin signaling has been shown to be accompanied by a mild oxidative burst. Upon activation of integrin signaling, ROS are generated from several sources including mitochondria, Nox, and lipooxygenases (LOX) (Taddei et al., 2007). Thus, released ROS trigger downstream signaling cascades by activating focal adhesion molecules. One of the most well-studied focal adhesion proteins is FAK, the principal kinase responsible for the formation of focal adhesion complexes (Ben Mahdi et al., 2000). Interactions between FAK and Src kinase have been implicated to play crucial roles in cell migration by phosphorylating the focal adaptor proteins PKC has been known to be involved in integrin signaling. Moreover, integrin signaling activates PKC, which in turn can signal back to activate integrins, suggesting the presence of a positive feedback mechanism between integrin and PKCs (Disatnik and Rando, 1999). Recently, ROS have been identified as an intermediate player in this loop. Translocation of PKC to the cell membrane activates integrin signaling that results in increased ROS levels. The ROS thus generated oxidize PKC and activate it. Thus, PKC-dependent integrin signaling generates ROS, which may in turn re-activate PKC, leading to sustained ERK activation and enhanced cell migration (Hu et al., 2011).

Cell invasion: Different types of cellular protrusions have been described during cell migration, including filopodia, lamellipodia, and invadopodia. Formation of specific protrusions is regulated by signalling pathways; for example, Rho activation induces filopodia and stress fiber formation, while induction of Rac leads to the formation of

lamellipodia and membrane ruffles (Nobes and Hall, 1999). These cellular protrusions are affected by dynamic alterations in the cytoskeleton such as actin cytoskeleton, which in turn is controlled by signaling molecules such as Rac. Rac has been identified as an upstream regulator of the ROS-producing enzyme Nox, indicating that a pathway exists for ROS-regulation of the actin cytoskeleton.

Epithelial-to-mesenchymal-transition. EMT encompasses a number of cellular changes that permit epithelial cells to attain a mesenchymal phenotype. This is accompanied by loss of epithelial markers (including E-cadherin, laminin 1, ZO-1, cytokeratin, and collagen IV), induction of mesenchymal markers (such as N-cadherin and vimentin) and upregulation of transcription factors (including Snail, Slug, Twist, NF-κB, and Zeb). EMT is accompanied by aggressive behavior favoring invasion and metastasis of many cancer types. ROS have been widely documented to participate in induction of EMT in cancer, through the activation of Snail (Cannito et al., 2008). On the other hand, Snail has also been shown to regulate ROS levels, as Snail overexpression in prostate cancer increases intracellular ROS levels (Barnett et al., 2011). This suggests a possible feedback mechanism by which ROS and Snail can regulate each other and more importantly, both events leading to induction of EMT.

Expression of genes implicated in hypoxia-induced EMT and angiogenesis may also be regulated by ROS. The transcription factor hypoxia inducible factor 1-alpha (HIF-1α) is induced by hypoxia and in turn activates downstream transcription of EMT-related genes. Interestingly, under hypoxic stress, ROS are produced due to aberrant function of mitochondrial complex III (Giannoni et al., 2012), thus stabilizing HIF-1 by oxidative inhibition of the HIF-degrading enzyme prolyl hydroxylase. Moreover, under hypoxic conditions, EMT-related events such as translocation of Snail to the nucleus are found to be determined by the amount of intracellular ROS levels (Cannito et al., 2008).

Mounting evidence also suggests the influence of TGF-beta induced ROS in EMT-mediated cellular changes. As a multi-potent cytokine, TGF-beta plays an important role in EMT and tumor progression. Several mechanisms by which TGF-beta induces EMT via regulation of intracellular ROS have been proposed. TGF-beta has been shown to increase ROS levels by decreasing the expression and activity of the antioxidant protein Glutaredoxin (Grx1) (Lee et al., 2010). In mammary epithelial cells expressing oncogenic Ras, downregulation of Grx1 by TGF-beta leads to increased intracellular ROS levels promoting EMT. Moreover, increased ROS levels downstream of TGF-beta have been shown to activate signaling pathways such as MAPK leading to EMT (Felton et al., 2009).

MITOCHONDRIA

The general framework

The mitochondrion represents a unique organelle within the complex endomembrane systems that characterize any eukaryotic cell. Beyond the pivotal role they play in ATP production, a whole new mitochondrial biology has emerged in the last few decades: mitochondria have been shown to participate in many other aspects of cell physiology such as amino-acid synthesis, iron-sulphur clusters assembly, lipid metabolism, Ca2+ signaling, reactive oxygen species (ROS) production and cell death regulation.

Hence, many pathological conditions are associated with mitochondria dysfunction, including neurodegenerative diseases (Alzheimer's, Parkinson's, Hungtinton's), motoneuron disorders (amyotrophic lateral sclerosis, type 2A Charcot-Marie-Tooth neuropathy), autosomal dominant optic atrophy, ischemia-reperfusion injury, diabetes, ageing and cancer (Duarte et al., 2014; Gaude and Frezza, 2014).

Understanding how mitochondria can sense and decode various signals from the cytosol and other subcellular compartments represents a new exciting challenge in biomedical sciences.

Mitochondria are defined by two structurally and functionally different membranes: the plain outer membrane (OMM), permeable to ions and metabolites up to 5000 Da, and the highly selective inner membrane (IMM), characterized by invaginations called *cristae* which enclose the mitochondria matrix. The space between the two membranes is called intermembrane space (IMS). The cristae define internal compartments formed by profound invaginations originating from narrow tubular structures called *cristae junctions* (Mannella, 2006) that limit the diffusion of molecules from the intra-cristae space towards the IMS, thus creating a micro-environment where the mitochondrial Electron Transport Chain (mETC) complexes are hosted and other proteins are protected from random diffusion.

Mitochondrial Ca^{2+} signaling

Mitochondria can rapidly accumulate Ca^{2+} down the electrochemical gradient established by the translocation of protons across the inner mitochondrial membrane (IMM), which is expressed as a membrane potential difference ($\Delta\Psi_m$) of -180mV (negative inside) under physiological conditions (Mitchell, 1966). However, the accurate measurements of $[Ca^{2+}]$ in resting cells revealed values well below the affinity of the mitochondrial transporters. Thus, the role of mitochondria in Ca^{2+} homeostasis was considered marginal (i.e. limited to conditions of cellular Ca^{2+} overload), till the development of specific and reliable probes directly reported major swings of mitochondrial $[Ca^{2+}]$ even upon physiological stimuli (Rizzuto et al., 1992). While enlivening the interest in mitochondrial Ca^{2+} homeostasis, these data raised an apparent contradiction between the prompt accumulation of Ca^{2+} under physiological stimulations and the low affinity of the mitochondrial Ca^{2+} uniporter, the highly selective channel responsible for Ca^{2+} entry into the mitochondrial matrix, at both resting and agonist-stimulated $[Ca^{2+}]_{cyt}$.

Based on a large number of experimental proofs, it is now clear that the key of the rapid Ca^{2+}_{mit} accumulation resides in the strategic location of mitochondria in close proximity to ER-resident Ca^{2+} channels and implies the assembly of a dedicated signalling unit at the interface of the two organelles. By labelling mitochondria and ER with targeted spectral variants of GFP (mtGFP and erGFP) the presence of overlapping regions of the two organelles, called “mitochondria-associated membranes” (MAM) has been revealed and the area of the contact sites has been estimated as 5-20% of the total mitochondrial surface (Rizzuto et al., 1998). The idea of local Ca^{2+} microdomains between the mitochondria and the ER, was further demonstrated by Rizzuto et al., by fast single-cell imaging of $[Ca^{2+}]_{mit}$ with targeted Ca^{2+}-sensitive GFPs (pericams and cameleons), which showed that $[Ca^{2+}]_{mit}$ increases originate from a discrete number of ER-sites and then rapidly diffuse through the mitochondrial network.

Mitochondrial Ca^{2+} regulation of cellular energetics, cell death and autophagy.

As mentioned before, mitochondria are the main site of ATP production. When glucose is converted to pyruvate by glycolysis, only a small fraction of the available chemical energy has been stored in ATP molecules: mitochondria can "release" the remaining amount of energy with an outstanding efficiency (from a single glucose molecule, mitochondria produce 15 times more ATP than glycolysis). The main enzymatic systems involved in this process are the tricarboxylic acid (TCA) cycle and the mETC. Products from glycolysis and fatty acid metabolism are converted to acetyl-CoA which enters the TCA cycle where it is fully degraded to CO_2. More importantly, these enzymatic reactions generate NADH and FADH2 which provide reducing equivalents and trigger the electron transport chain. mETC consists of five different protein complexes: complex I (NADH dehydrogenase), complex II (succinate dehydrogenase), complex III (ubiquinol cytochrome c reductase), complex IV (cytochrome c oxidase) and complex V that constitutes the F_1F_0-ATP synthase. Electrons are transferred from NADH and FADH2 through these complexes in a stepwise fashion: as electrons move along the respiratory chain, energy is stored as an electrochemical H+ gradient across the inner membrane, thus creating a negative mitochondrial membrane potential (estimated around -180 mV against the cytosol). H+ are forced to re-enter into the matrix mainly through complex V, which couples this proton driving force to the phosphorylation of ADP into ATP, according to the chemiosmotic principle. ATP is then released to IMS through the electrogenic Adenine Nucleotide Translocase (ANT), which exchanges ATP with ADP to provide new substrate for ATP synthesis. Finally, ATP can easily escape the IMS thanks to the mitochondrial porin of the outer membrane, VDAC (voltage dependent anion channel) (Duchen, 2004).

A complex Ca^{2+}-sensing machinery, localized in different mitochondrial domains, underlies the coupling of aerobic metabolism to Ca^{2+}-mediated signals in the cytosol. In detail, the main physiological role of mitochondrial Ca^{2+} uptake is the control of ATP production rate. Indeed, important enzymes of the TCA cycle, i.e. pyruvate-, α-ketoglutarate- and isocitrate-dehydrogenases (collectively called the Ca^{2+}-sensitive mitochondrial dehydrogenases, CSMDHs) are activated by Ca^{2+}, with different mechanisms: the first through a Ca^{2+}-dependent dephosphorylation step, the others via direct binding to a regulatory site (McCormack et al., 1990). Those three enzymes represent rate-limiting steps of the Krebs cycle thus controlling the feeding of electrons into the respiratory chain and the generation of the proton gradient across the inner membrane, in turn necessary for ATP production.
Moreover, other Ca^{2+}-dependent mechanisms control mitochondrial metabolism. Indeed, metabolite carriers of the inner membrane, such as Aralar1 and Citrin, possess a Ca^{2+} binding site in the portion of the protein protruding in the intermembrane space, which is responsible for substrate accumulation into the matrix (Lasorsa et al., 2003).

The growing interest in the molecular processes of Ca^{2+}_{mit} homeostasis further prompted to understand increased how programmed cell death (i.e. apoptosis) might be causally linked to organelle Ca^{2+} loading. Indeed, Ca^{2+} sensitizes cells to apoptotic challenges, acting on the mitochondrial checkpoint. Ca^{2+} binding to Cyclophilin-D positively regulates PTP opening (Basso et al., 2005). Once opened, PTP allows the release in the cytosol of intermembrane-residing apoptotic factors, such as cytochrome C, AIF (apoptosis inducing factor) and Smac/DIABLO, which can trigger apoptosis by both a caspase-dependent and a caspase-independent pathway (Giorgi et al., 2008). Physiological $[Ca^{2+}]_{mit}$ oscillations do not induce PTP opening, but become effective with the synergistic action of pro-apoptotic challenges (such as ceramide or staurosporin) (Pinton et al., 2001).

Another fundamental Ca^{2+}_{mit}-dependent process concerns the control of autophagy. Recent reports describe Ca^{2+} as an inhibitor of autophagy. In 2005, Sakar et al. reported the use of Li^{+} for autophagy stimulation, through inhibition of inositol monophosphatase (IMPases), by reducing the IP3 levels (Sarkar et al., 2005). Also chemical inhibition of IP3Rs with xestospongin (XeB) or suppression of its expression using siRNA, enhanced autophagy in HeLa cells (Criollo et al., 2007). Different downstream mechanisms and effectors have been proposed for the inhibitory role of IP3Rs-released Ca^{2+} in autophagy. In a recent study, Cardenas and coworkers showed increased glucose and O_2 consumption, as well as PDH and AMPK activation in IP3Rs -KO cells, suggesting that constitutive Ca^{2+} release, through IP3Rs, fueling into the mitochondria, increases mitochondrial bio-energetics and ATP production, thus suppressing autophagy. When the physiological Ca^{2+}mit uptake is abolished, an increase in the AMP/ATP ratio is registered, with a consequent AMPK activation, which stimulates autophagy (Cardenas et al., 2010).

Moreover, cell treatments with ER/SR Ca^{2+} ATPase (SERCA) inhibitors resulted in increased autophagy (Hoyer-Hansen and Jaattela, 2007).

Mitochondrial Ca2+ Uniporter Complex: molecular identity and regulation.

The fruitful investigation of the molecular identity of the Mitochondrial Calcium Uniporter (MCU) took advantage of a genome-wide approach. In 2008, Mootha and co-workers reported a mitochondrial “genoteque” called MitoCarta. It was obtained by performing mass spectrometry analyses, on both highly purified and crude mitochondrial preparations, from 14 different mouse tissues, in order to discover genuine mitochondrial proteins, further validated by GFP tagging (Pagliarini et al., 2008). By considering only those proteins localized in the IMM, expressed in the majority of mammalian tissue and with homologues in

vertebrates and kinetoplastids (but not in yeast), they identified a protein named "Mitochondrial Calcium Uptake 1" (MICU1). MCU1 possesses one transmembrane domain and two canonical EF-hands, essential for Ca^{2+}-sensing. MICU1 was thus recognized as a modulator of the Mitochondrial Calcium Uniporter (MCU) (Perocchi et al., 2010).

The MitoCarta database and the molecular identification of MICU1 set the basis for the subsequent identification of MCU. Accordingly, the Mitocarta database was examined with unbiased search constraints, on the basis of the phylogenetic appearance of Ruthenium Red-sensitive Ca^{2+} uptake (which excluded the yeast proteome, but included the kinetoplastid proteome), tissue distribution (which should be ubiquitous in the case of the MCU) and by minimal sequence requirements for channels (i.e. the existence of two or more transmembrane domains (TMDs)). Finally, our and Mootha's labs identified a protein, encoded by the CCDC109A gene, which satisfies all the requirements of the *bona fide* Mitochondrial Calcium Uniporter (Baughman et al., 2011; De Stefani et al., 2011). MCU overexpression in HeLa cells strongly increases Ca^{2+}_{mit} uptake while its silencing by siRNA drastically reduces it. Importantly, Baughman et al. demonstrated *in vivo* that knockdown of MCU in liver triggers complete inhibition of Ca^{2+}_{mit} uptake in response to extramitochondrial pulses of Ca^{2+}. De Stefani et al. demonstrated that MCU is necessary and sufficient to mediate Ca^{2+} uptake. Indeed, purified MCU formed a RuR-sensitive channel in planar lipid bilayers.

In 2012, Mallilankaraman K. and coworkers demonstrated that MICU1 is required to preserve basal mitochondrial [Ca^{2+}] levels. Indeed, in its absence mitochondria are constitutively loaded with Ca^{2+}, thus triggering excessive reactive oxygen species generation and sensitivity to apoptotic stimuli (Mallilankaraman et al., 2012b). Additional publications, identified other components of the MCU complex, confirming the hypothesis that MCU is a

multisubunit channel, with associated regulators, which partecipate in the tightly regulation of the pleiotropic Ca^{2+}_{mit} functions.

In 2012, Raffello and coworkers characterized a novel protein, named MCUb, with two predicted transmembrane domains, 50% sequence similarity with MCU but a different expression profile. Based on computational modelling, MCUb includes critical amino-acid substitutions in the pore region and therefore MCUb does not form a calcium-permeable channel in planar lipid bilayers. In HeLa cells, MCUb is part of the MCU oligomer and exerts a dominant-negative effect, reducing the $[Ca^{2+}]_{mit}$ increase evoked by agonist stimulation (Raffaello et al., 2013).

Furthermore, Mallilankaraman and coworkers identified a new important component of this complex. Indeed, they showed that the MCU-regulator 1 (MCUR1) is an IMM integral membrane protein, required for MCU-dependent mitochondrial Ca2+ uptake. Furthermore, they showed that this protein is involved in the regulation of oxidative phosphorylation and in the activation of AMPK dependent pro-survival autophagy (Mallilankaraman et al., 2012a). However, a recent publication of Paupe et al. demonstrated that MCUR1 is a Cytochrome C oxidase assembly factor and not a regulator of the Mitochondrial Calcium Uniporter (Paupe et al., 2015).

In MICU1-silenced cells, MICU2 is also eliminated and mitochondrial Ca^{2+} gatekeeping is abolished, in agreement with previous reports (Csordas et al., 2013; Mallilankaraman et al., 2012b). At low $[Ca^{2+}]$, the dominant effect of MICU2 largely shuts down MCU activity; at higher $[Ca^{2+}]$, the stimulatory effect of MICU1 allows the prompt response of mitochondria to Ca2+ signals generated in the cytoplasm. In 2014, an additional work demonstrated that, a protein coded MICU2, is the genuine gatekeeper of MCU (Patron et al., 2014). Indeed,

MICU2 inhibits the channel activity of purified MCU in planar lipid bilayers and, accordingly, reduces channel opening at resting [Ca^{2+}], in intact HeLa cells. MICU2 forms an obligate heterodimer with MICU1, located in the mitochondrial intermembrane space.

Finally, a 10-kilodalton, metazoan-specific protein, with a single transmembrane domain, has been identified. In its absence, uniporter channel activity is lost, despite intact MCU expression and oligomerization; thus, the name "Essential MCU Regulator" (EMRE). EMRE seems to be required for the interaction of MCU with MICU1 and MICU2. Hence, EMRE is essential for uniporter current and regulates the calcium-sensing role of MICU1 and MICU2 on MCU conductance (Sancak et al., 2013).

MCU role in cancer progression

Recently, the role of MCU in cancer has been explored. The molecular characterization of the MCU protein complex opened the intriguing chance to modulate mitochondrial function by modifying MCU channel's activity. This possibility could become even more challenging if translated into the intricate background cancer pathophysiology, since little is known about the contribution of Ca^{2+}_{mit} to tumor progression.

Prostate and colon cancers overexpress a MCU-targeting microRNA that, by reducing mitochondrial Ca^{2+} uptake, favors cancer cell resistance to apoptotic stimuli, thus increasing cell survival (Marchi et al., 2013). Knockdown of MICU1 triggers an increased mROS generation thus enhancing the sensitivity of HeLa cells to ceramide-induced cell death (Mallilankaraman et al., 2012b).

In the highly malignant triple negative breast cancer MDA-MB-231 cell model, MCU silencing potentiated a caspase-independent cell death triggered by ionomycin, suggesting that MCU

overexpression may offer a survival advantage against some apoptotic pathways (Curry et al., 2013).

A recent report pointed out a striking correlation between MCU gene overexpression and MICU1 underexpression from breast cancer samples with significantly poorer prognosis outcomes. Nonetheless, in the highly aggressive triple negative MDA-MB-231 breast cancer cell line, no relevant changes in ROS levels or in cell survival, after both inhibition and activation of MCU, were reported (Hall et al., 2014).

AIM

Mitochondrial dysfunction is common to many pathological conditions, including cancer. Tumor cells frequently exhibit disease-promoting traits linked to alterations in mitochondrial function, including increased glycolysis and Reactive Oxygen Species (ROS) production, and resistance to apoptotic stimuli.

Triple Negative Breast Cancer (TNBC), a clinically heterogeneous category of tumors that lack expression of estrogen, progesterone and HER2 receptors, show profound metabolic alterations with impaired mitochondrial oxidative metabolism (Elias, 2010; Owens et al., 2011). However, very little is known about mitochondrial Ca^{2+} regulation or its signaling in these tumorigenic settings.

Metastatic breast cancer cells respond promptly to agonist stimulation, by accumulating much higher [Ca^{2+}] into the mitochondrial matrix, compared to premalignant cells. On this basis, we hypothesized alternative roles of mitochondrial Ca^{2+}, distinct from those of non-tumor cells (i.e. mitochondrial energy production and control of cell death) possibly involved in the metastatic progression of TNBC.

We took advantage of the molecular characterization of the Mitochondrial Calcium Uniporter (MCU), the highly selective channel responsible for Ca^{2+} entry into the mitochondrial matrix, to investigate whether, by reducing Ca^{2+}_{mit} uptake, metastatic TNBC properties, such as cell migration and matrix invasiveness, are affected.

Then, we focused on mitochondrial Reactive-Oxygen-Species (mROS) production. Indeed, mROS molecules are crucial molecular effectors for cancer cell progression, by eliciting both metabolic adaptations and in vivo metastasis formation (Porporato et al., 2014; Tochhawng

et al., 2013). Accordingly, we aimed at investigating whether Ca^{2+}_{mit} uptake modulates mROS production, thus contributing to the regulation of intracellular ROS-dependent pathways. Finally, aiming at understanding the molecular effector translating Ca^{2+}-dependent ROS signalling into a metastatic phenotype we focused on hypoxia-inducible-factor-1α (HIF-1α), the transciption factor responsible for many metastasis-related genes expression. Our study highlights an unexpected, intriguing regulation exerted by MCU on HIF-1α.

RESULTS

MCU suppression impairs TNBC cell migration.

In order to decipher the role of mitochondrial Ca^{2+} signaling in TNBC metastatic potential, we took advantage of the MCF10 system of breast cell lines. We first compared the mitochondrial Ca^{2+} uptake responses of premalignant versus malignant cells. Upon agonist stimulation, the highly metastatic MCF10CA1a.cl1 transiently accumulated significantly higher [Ca^{2+}] than the premalignant MCF10AT1Kcl.2 (Fig. 1a). We hypothesized that high $Ca^{2+}{}_{mit}$ transients, while sensitizing premalignant cells to pro-apoptotic stimuli, may be instrumental for metastatic progression.

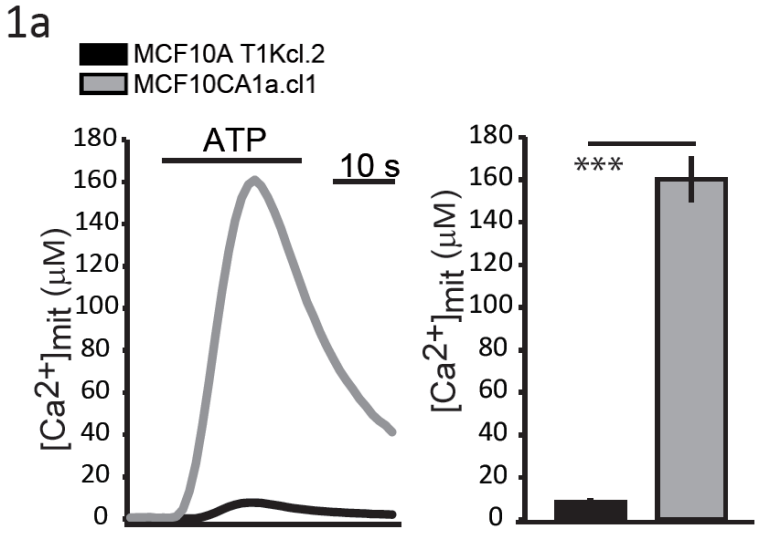

FIG.1a. **Metastatic cells accumulate higher $[Ca^{2+}]_{mit}$ than premalignant cells upon agonist stimulation.** Metastatic (MCF10CA1a.cl.1) and premalignant (MCF10AT1kcl.2) cell lines were infected with Ad-mitAeqMUT, as $Ca^{2+}{}_{mit}$ indicator. $[Ca^{2+}]_{mit}$ uptake upon ATP stimulation was measured (n= 6, ***p<0.001).

Accordingly, three different metastatic Triple Negative Breast Cancer (TNBC) cell lines were analyzed, i.e. BT-549, MDA-MB-468 and MDA-MB-231. In all three models, as expected, short interfering RNA (siRNA)-mediated inhibition of the Mitochondrial Calcium Uniporter (MCU), the highly selective channel responsible for Ca^{2+} entry into the mitochondrial matrix, caused a significant decline in agonist-induced $[Ca^{2+}]_{mit}$ uptake (Fig.1b-d).

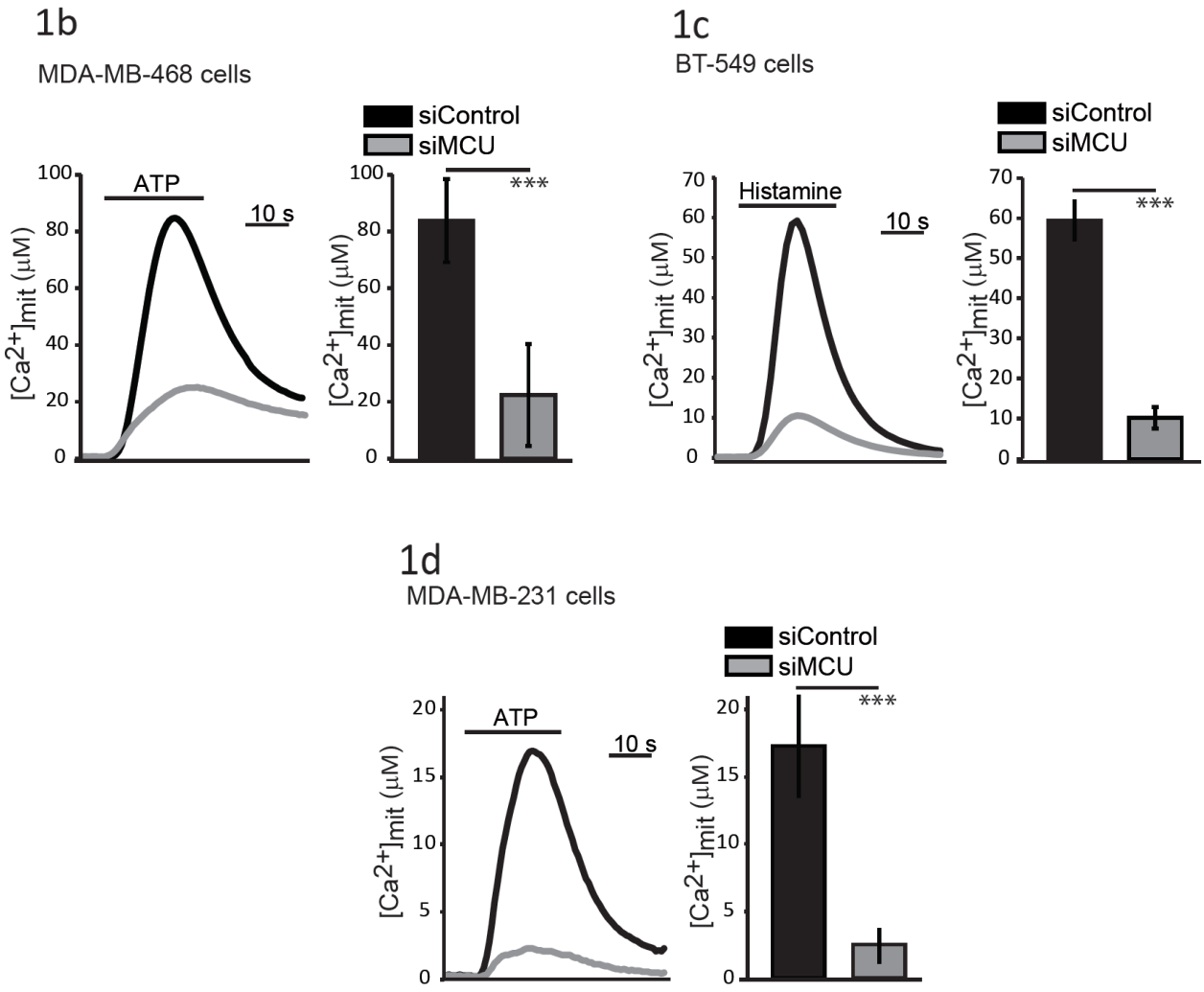

FIG.1b-d. **MCU silencing critically reduces Ca^{2+}_{mit} uptake in TNBC cells**. Cells were transfected with siMCU or siControl. After 48h, $[Ca^{2+}]_{mit}$ uptake upon ATP (Fig.1b, 1d) or Histamine (Fig.1c) stimulation was measured (n=6, ***p< 0.001).

Moreover, MCU silencing impaired TNBC cells motility, monitored by wound healing migration assay (FIG.1e-g).

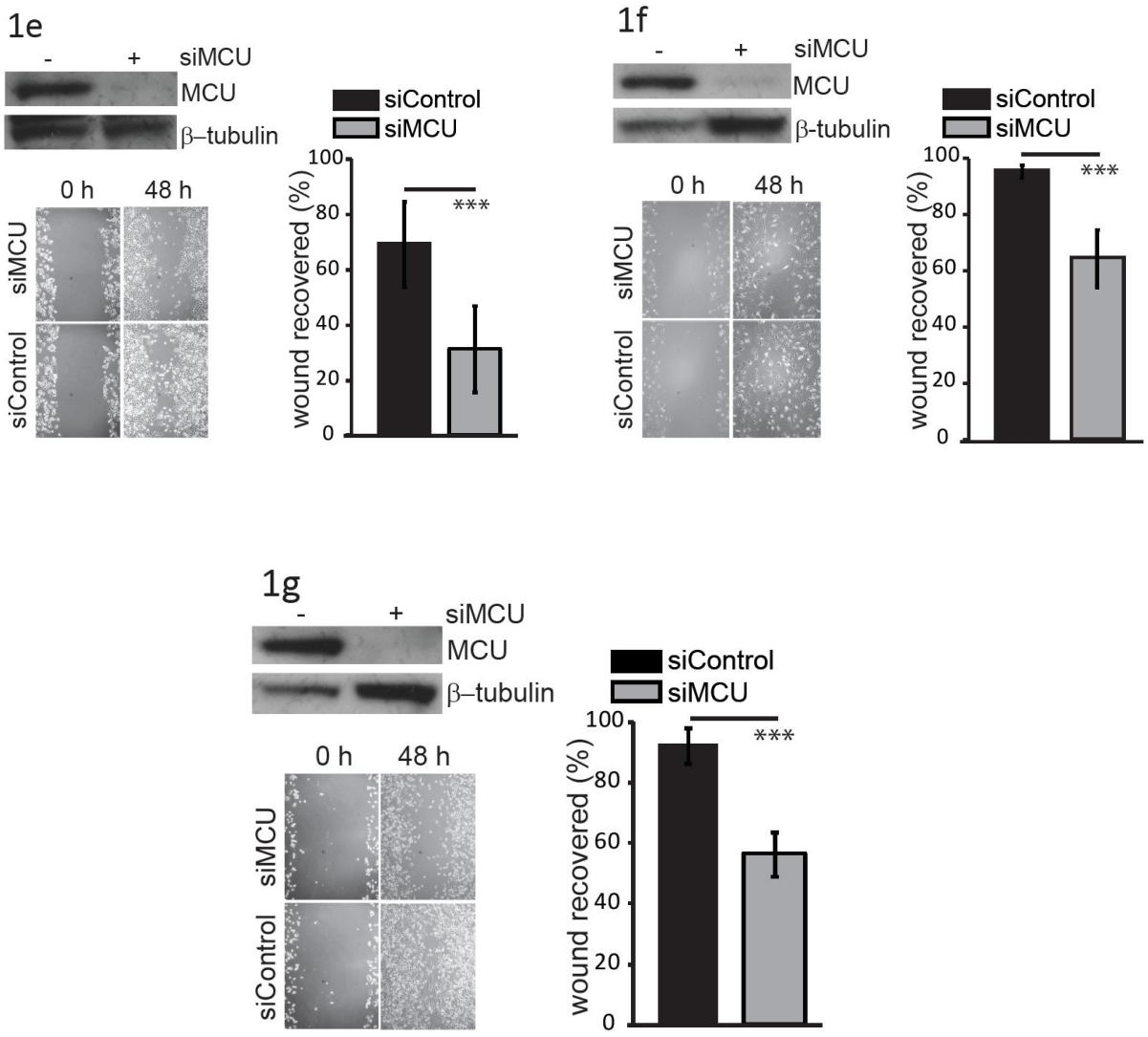

FIG.1e-g. **MCU silencing impairs TNBC cell migration**. MDA-MB-468 (Fig.1e), BT-549 (Fig.1f), MDA-MB-231 (Fig.1g) cells were transfected with siMCU or siControl. The day after transfection cells were scratched with a vertically held tip (time point 0h). Cell migration into the wounded area was monitored at 48-hour time point. The recovered area was measured and expressed as a percentage relative to 0-hour time point (n=3, ***p<0.001).

Importantly, proliferation of BT-549 and MDA-MB-468 cells was unaffected by MCU silencing (Fig.1h and 1i). Of note, at 72 hours (which corresponds to the 48-hour time point of the wound healing assay) MDA-MB-231 cell growth was modestly but significantly inhibit by siMCU (Fig. 1j).

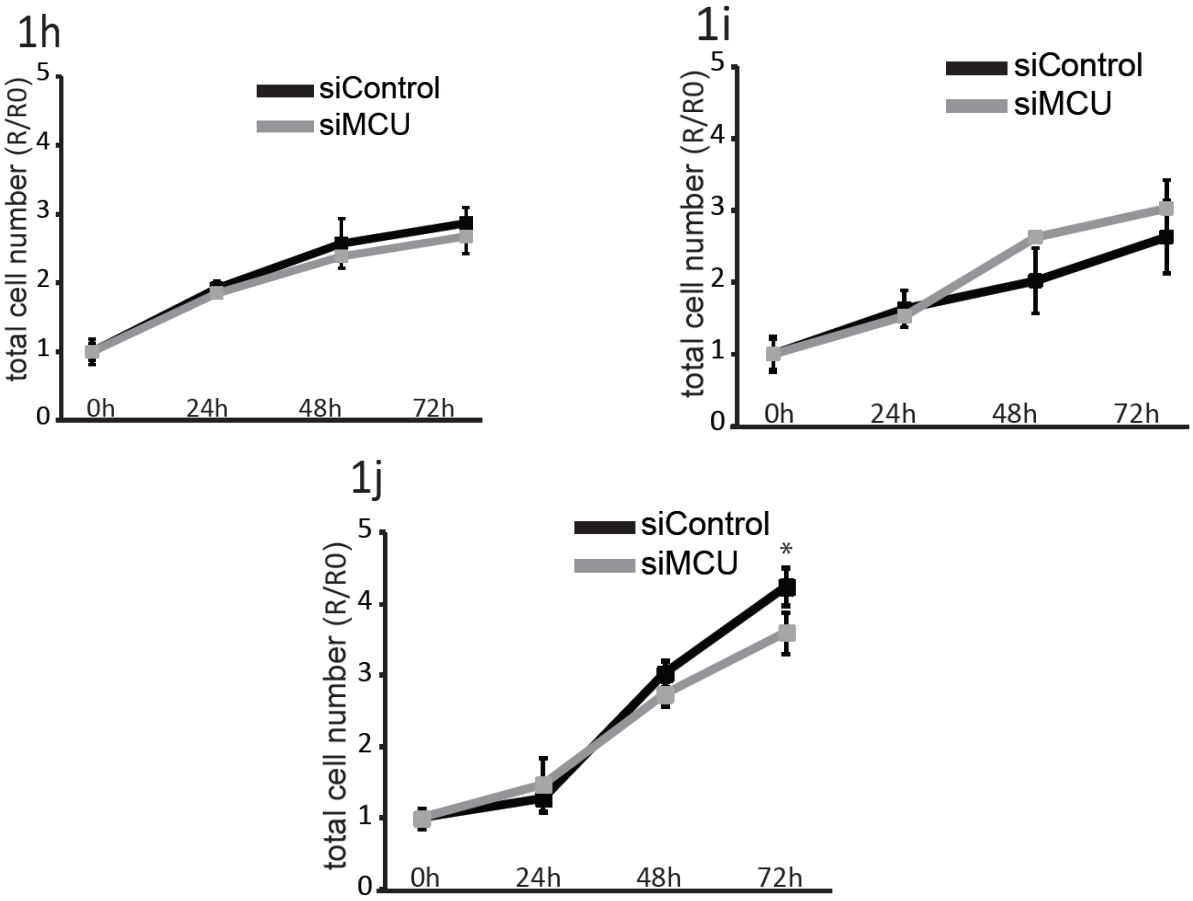

FIG.1h-j. **MCU depletion does not affect cell proliferation**. MDA-MB-468 (Fig.1h), BT-549 (Fig.1i), MDA-MB-231 (Fig.1j) cells were transfected with siMCU or siControl. Cell number was counted every 24 hours, for 3 days (the 72-hour time point corresponds to the 48-hour time point of wound healing assay). Results are expressed as ratio R/R0 where R0 is the number of cells at the time of transfection (0 hour-time point) (n=3, *p<0.05).

MCU silencing blunts cell invasiveness without affecting cell viability, nor reverting the mesenchymal phenotype

In order to further investigate the molecular mechanism involved in the regulation of migration by MCU, we selected MDA-MB-231 cells. Of note, re-expression of mMCU rescued cell motility in cells in which MCU was silenced, confirming the specificity of siMCU effects (Fig.2a).

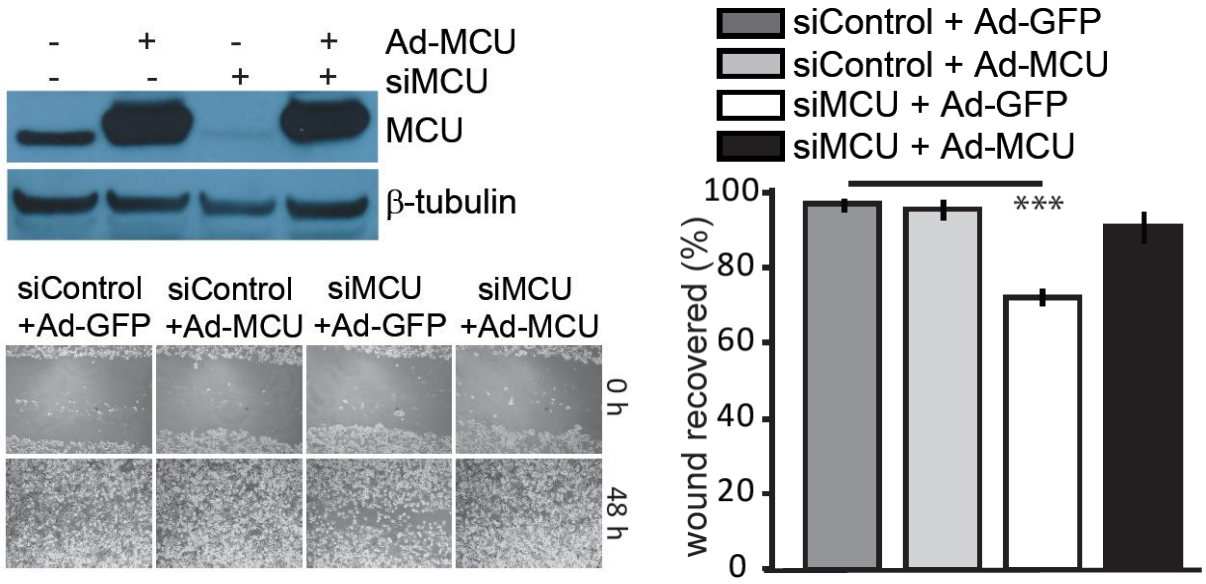

FIG.2a. Re-expression of mMCU rescues cell motility of MCU-silenced cells. Cells were transfected with siMCU or siControl. Ad-mMCU was used to re-express MCU (Ad-GFP as control). The day after transduction cells were scratched (time point 0h). Cell migration into the wounded area was monitored at 48 hour-time point and the recovered area was measured (n=6, ***p<0.001).

Then, we wished to confirm the data on migration obtained by siRNA transfection by a pharmacological approach. In agreement with siRNA data, KB-R7943, a specific MCU

inhibitor (Santo-Domingo et al., 2007) strongly reduced mitochondrial Ca^{2+} uptake (Fig.2b) and impaired migration (Fig.2c), indicating that both genetic and pharmacological inhibition of mitochondrial Ca^{2+} uptake are effective in controlling cell migration.

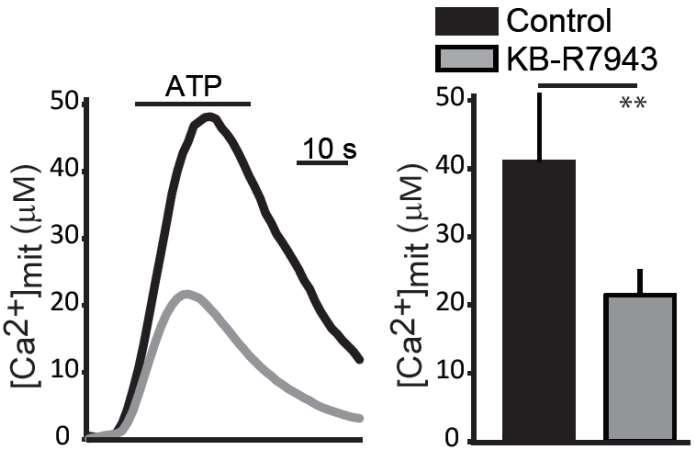

FIG.2b. **Pharmacological inhibition of MCU reduces Ca^{2+}_{mit} uptake of MDA-MB-231 cells, upon agonist stimulation.** Cells were treated for 48 hours with KB-R7943. Ca^{2+}_{mit} uptake after ATP stimulation was measured (n=6, **p<0.01).

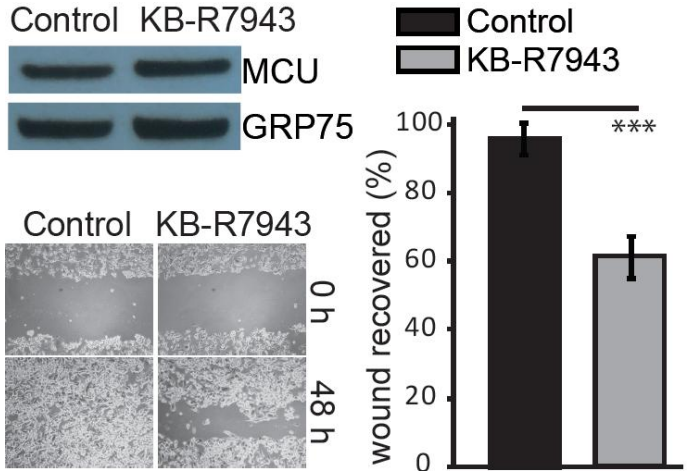

FIG.2c. Pharmacological inhibition of MCU impairs migration. A cell monolayer was scratched (0-hour time point) and treated for 48 hours with KB-R7943. Cell migration was monitored at 48-hour time point. (n=6, ***p< 0.001).

Next, the invasion potential of TNBC cells upon MCU silencing was investigated. For this purpose, an *in vitro* spheroid formation assay was performed by infecting MDA-MB-231 cells with a lentivirus expressing shMCU, demonstrating that 48 hours of MCU silencing deeply impairs the ability of TNBC cells to invade the surrounding collagen matrix (Fig.2d).

Of note, colony formation assay revealed that, in 7 days, cell growth was only partially inhibited by shMCU (Fig. 2e).

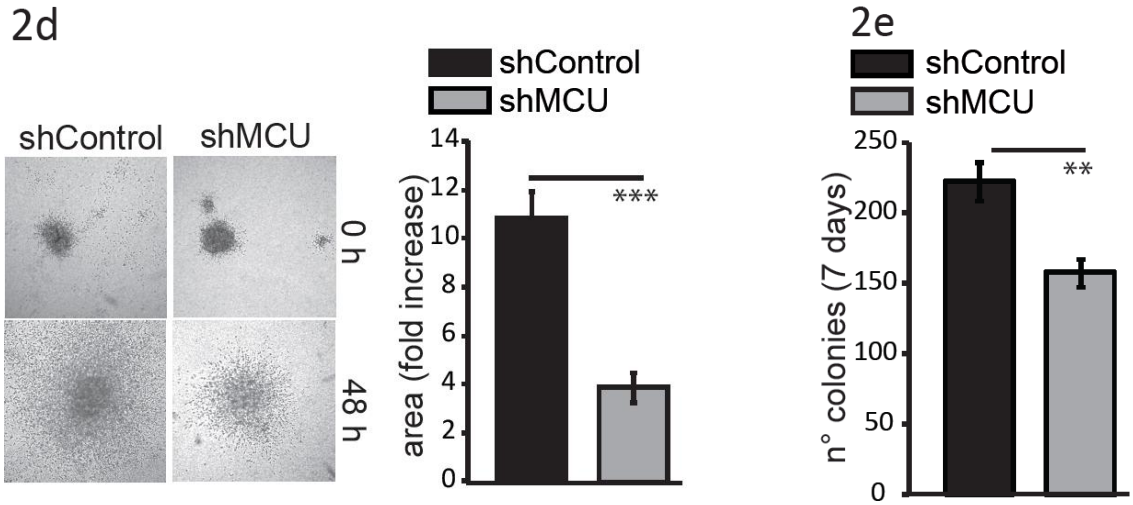

FIG.2d. **MCU silencing blunts cell invasiveness.** Stable shMCU and shControl-expressing spheroids were plated and let grow into collagen I (0-hour time point). The invasion of the surrounding matrix was monitored over time and expressed as final invaded area, relative to 0-hour time point (n=6, ***p<0.001).

FIG.2e. **MCU silencing reduces the clonogenic potential of MDA-MB-231 cells**. Stable shMCU and shControl-expressing cells were plated at low confluence ($2x10^3$/well of a 6-well plate) and let grow. After 7 days the number of colonies was counted (minimum 30 cells/colony, n=6, **p<0.01).

As already reported (Curry et al., 2013), we excluded a role of apoptosis and of cell cycle arrest in our experimental settings (Fig. 2f-2g). Moreover, the mesenchymal phenotype of MDA-MB-231 cells was not reverted to epithelial traits by MCU silencing, as demonstrated through the expression profile of the epithelial and mesenchymal markers (Fig.2h).

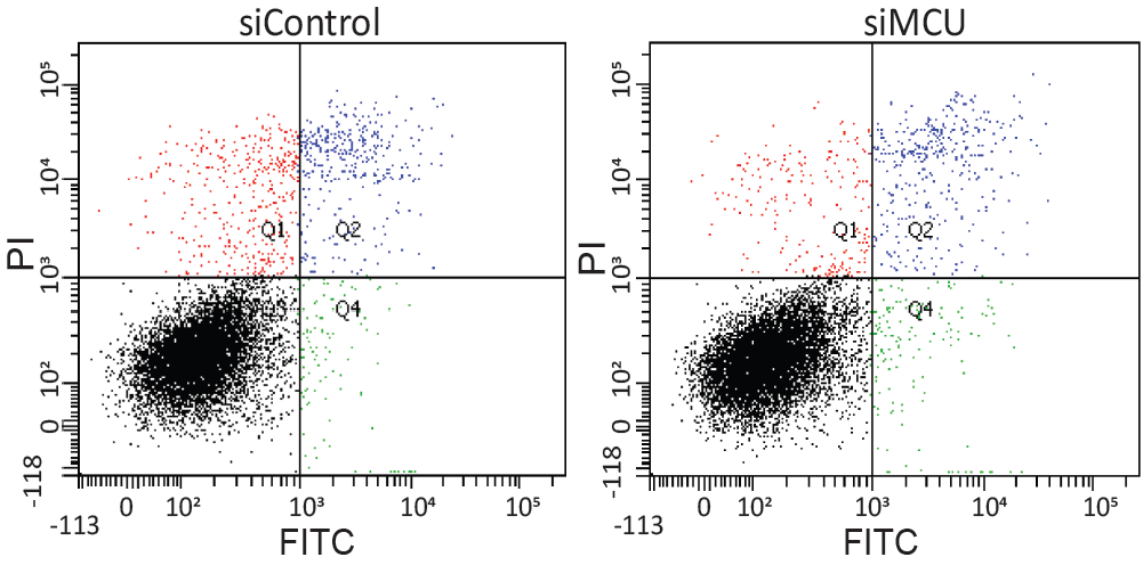

FIG.2f. MCU depletion does not induce apoptosis nor necrosis. Cells were transfected with siMCU or siControl. 72 hours after transfection cell apoptosis and necrosis was measured through FACS analysis, by loading samples with Annexin-V and Propidium Iodide (PI). (Q1: PI positive, Q2: PI and Annexin V positive, Q3: PI and Annexin V negative, Q4: Annexin V positive. n=4).

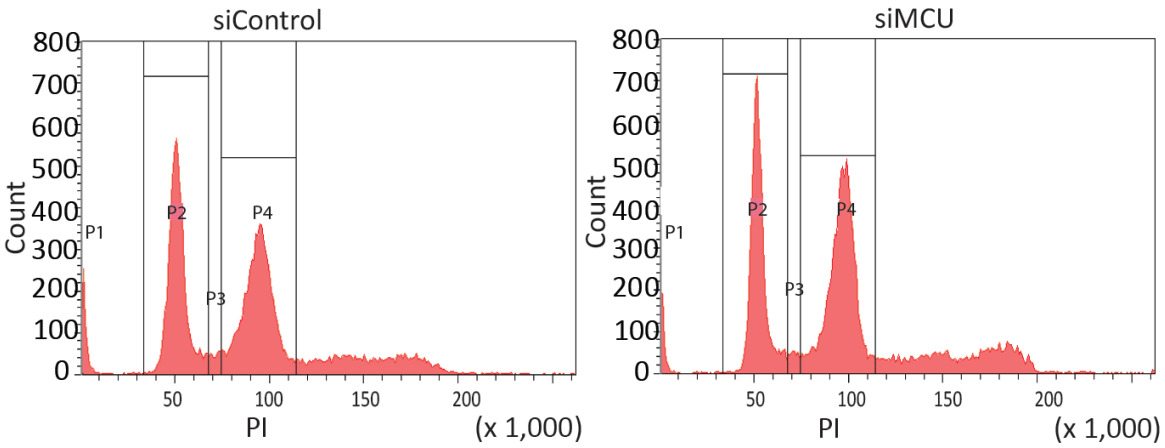

FIG.2g. **MCU depletion does not alter cell cycle.** Cells were transfected with siMCU or siControl. 72 hours after transfection cell cycle distribution was monitored through FACS analysis, by loading samples with Propidium Iodide (PI). (P1: G0 phase, P2: G1 phase, P3: S phase, P4: G2-M phase. n=4).

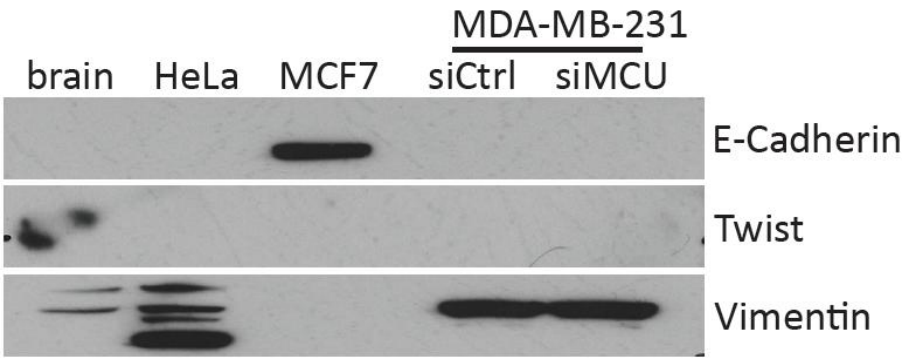

FIG.2h. MCU silencing does not revert the mesenchymal phenotype of MDA-MB-231 cells. Cells were transfected with siMCU or siControl. The expression profile of epithelial (E-Cadherin) and mesenchymal markers (Twist and Vimentin) was monitored by western blot. Mouse brain, HeLa and MCF7 cell lysates were used as positive controls.

MCU downregulation does not compromise mitochondria bioenergetics, although it impairs NAD(P)H production.

The drop in Ca^{2+}_{mit} uptake upon MCU silencing did not alter the mitochondrial membrane potential (Fig. 3a), neither affected mitochondrial oxidative phosphorylation capacity, since the Oxygen Consumption Rate did not significantly change (Fig. 3b). Nevertheless, we found a considerable decline in NAD(P)H production in cells stably expressing shMCU (Fig.3c), thus supporting the hypothesis that, although MDA-MB-231 cells are characterized by a preferentially glycolytic metabolism, the reduction of Ca^{2+}_{mit} uptake reduces also OXPHOS substrate.

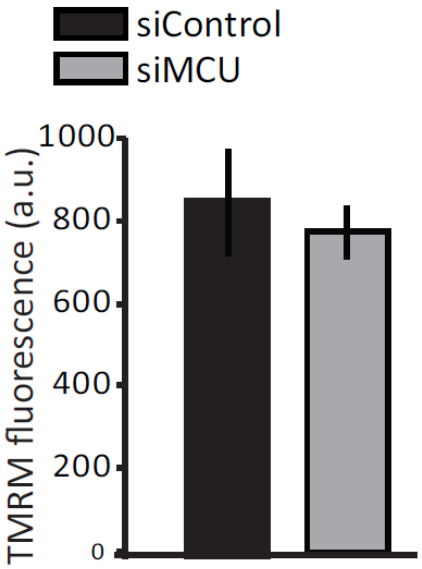

FIG.3a. MCU silencing does not compromise mitochondrial membrane polarization. Cells were transfected with siMCU or siControl. 48 hours after silencing, cells were loaded with tetramethylrhodamine ethyl ester (TMRE) and fluorescence was measured (n=3).

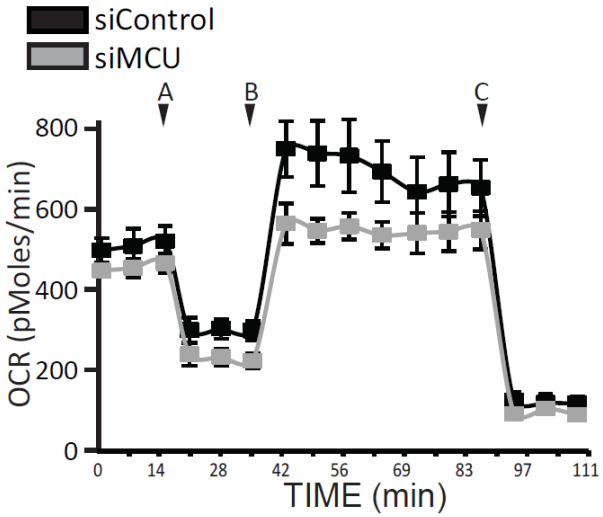

FIG.3b. MCU depletion does not alter oxygen consumption rate (OCR). Cells were transfected with siMCU or siControl. After 72h of MCU silencing oxygen consumption rate (OCR) was measured by means of a Seahorse-XF Analyzers. Mitochondrial respiration was first inhibited by addition of Oligomycyn (point A), then prompted by FCCP (point B) and finally dropped by Rotenone (point C) (n=3).

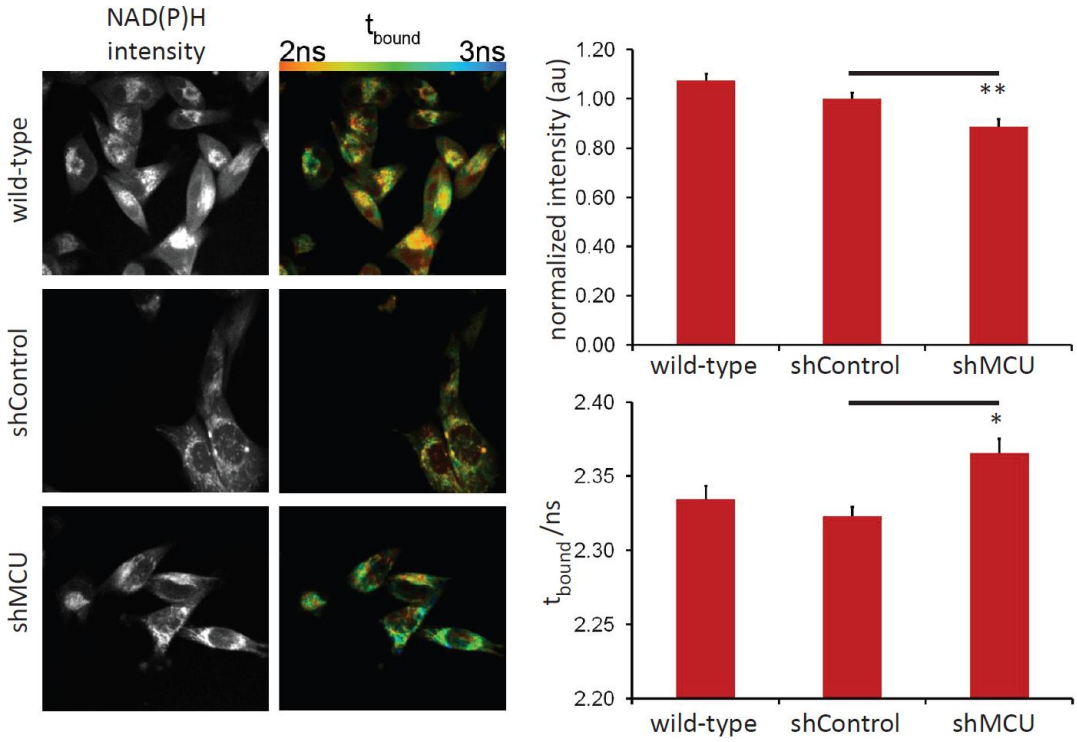

FIG.3c. **MCU silencing reduces NAD(P)H/NADH ratio**. NAD(P)H and NADH fuorescence of stable shMCU and shControl-expressing cells was analyzed. NAD(P)H/NADH ratio was measured according to the equation that correlates NADPH fluorescence decay with NADPH/NADH ratio (Blacker et al., 2014): $t_{bound}=(t_{NADPH}-t_{NADH})$ * ([NADPH]/([NADH]+[NADPH])+t_{NADH} (n=3, * p<0.05, **p<0.01).

Mitochondrial ROS production is critically reduced after MCU silencing.

We next ought to identify the molecular effectors of the migration inhibition mediated by MCU silencing. We focused on the role of mitochondrial Reactive Oxygen Species (ROS) since they represent signalling molecules that translate mitochondrial inputs into different cell responses, including cancer cell migration and invasion (Sena and Chandel, 2012; Tochhawng et al., 2013). Antioxidant molecules have been proposed as inhibitors of cell motility, both *in vitro* and *in vivo* (Porporato et al., 2014). Treatment with two different antioxidants, N-Acetylcysteine (NAC) and Dithioerythritol (DTE), revealed a dose-dependent impairment on migration, measured by wound healing assay (Fig. 4a). In order to specifically analyze the role of ROS produced by mitochondria on migration, we thought to validate this finding by means of a superoxide scavenging molecule specifically targeted to mitochondria, named MitoTEMPO. Migration assays of MitoTEMPO treated cells gave similar results, supporting the idea that mitochondrial ROS play a crucial role in TNBC migration (Fig. 4b).

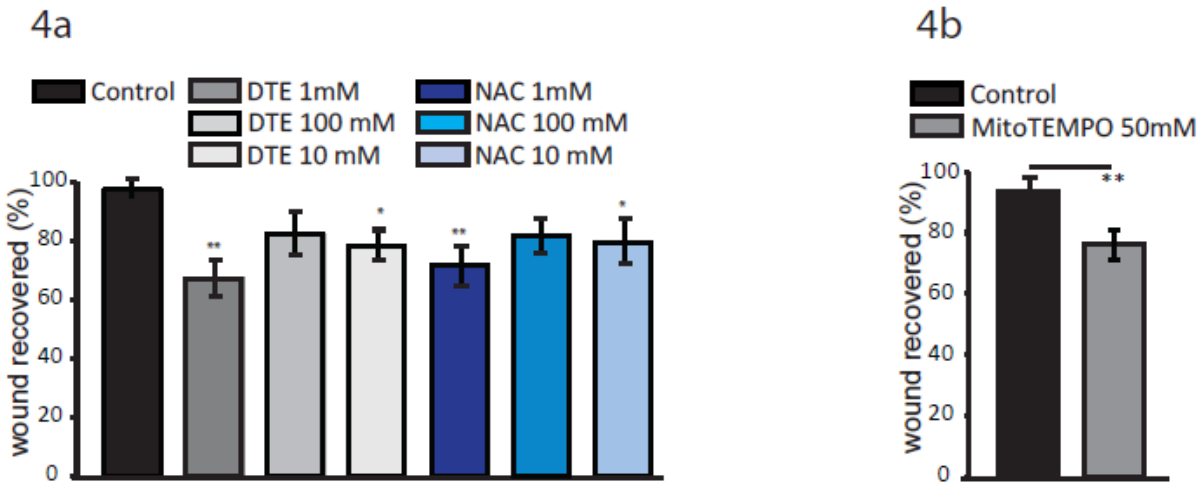

FIG.4a-b. **Antioxidant treatments decreases cell migration**. A cell monolayer was scratched (0 hour-time point) and treated for 48 hours with N-Acetylcysteine (NAC) or Dithioerythritol (DTE) (Fig.4a) or with MitoTEMPO (Fig.4b). Cell migration into the wounded area was monitored at 48-hour time point and the recovered area was measured (n=4, *p<0.05, **p<0.01).

Next, we verified the role of mitochondrial Ca^{2+} uptake on ROS production.

We took advantage of ectopic expression of $_{mit}$GRX1-roGFP2, a genetically encoded fluorogenic reduction-oxidation-sensitive GFP probe, to specifically measure mitochondrial glutathione redox potential (E_{GSH}), as a direct indication of oxidative stress. Live cell imaging revealed that MCU silencing caused a marked reduction in GSSG/GSSH ratio (Fig.4c). We confirmed this evidence with pHyper-dMito probe, a yellow fluorescent protein (YFP)-based biosensor specific for hydrogen peroxide, which showed a reduced mitochondrial H_2O_2 level in siMCU cells. One of the major advantages of these two redox sensitive probes is that they are ratiometric by excitation, thus limiting measurement errors deriving from photobleaching or concentration variability (Belousov et al., 2006; Gutscher et al., 2008).

Furthermore, we supported these results with two different non-ratiometric redox indicators, the mitochondrial H_2O_2-sensitive HyPerRed probe (Ermakova et al., 2014) and the red superoxide anion sensitive dye, MitoSOX^{TM} (Fig.4e and 4f).

All together these results highlight a significant reduction in mitochondrial ROS production by MCU silencing, suggesting that ROS may represent the key signaling mediators of MCU-regulated cell motility

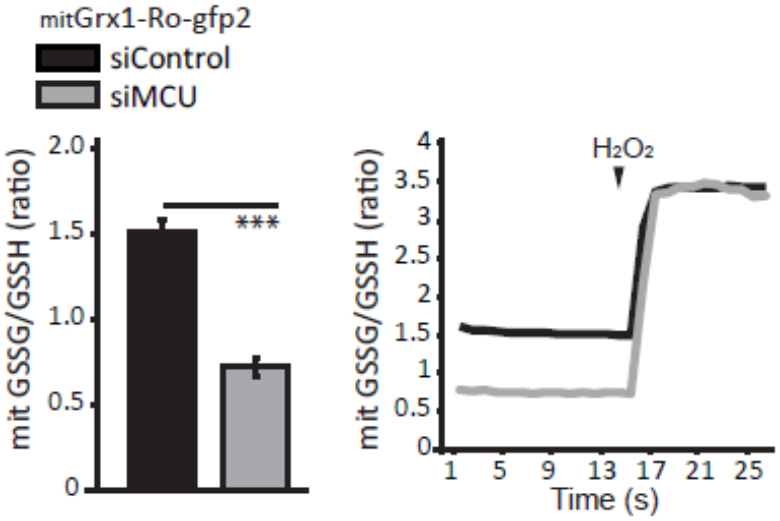

FIG.4c. Mitochondrial GSSG/GSSH ratio is critically reduced after MCU silencing. Cells were transfected with siMCU or siControl, together with the mitochondrial targeted mitGrx1-Ro-gfp2 probe. 48 hours after transfection the glutathione redox potential (E_{GSH}) was measured. H_2O_2 was added as a positive control (n=4, ***p<0.001).

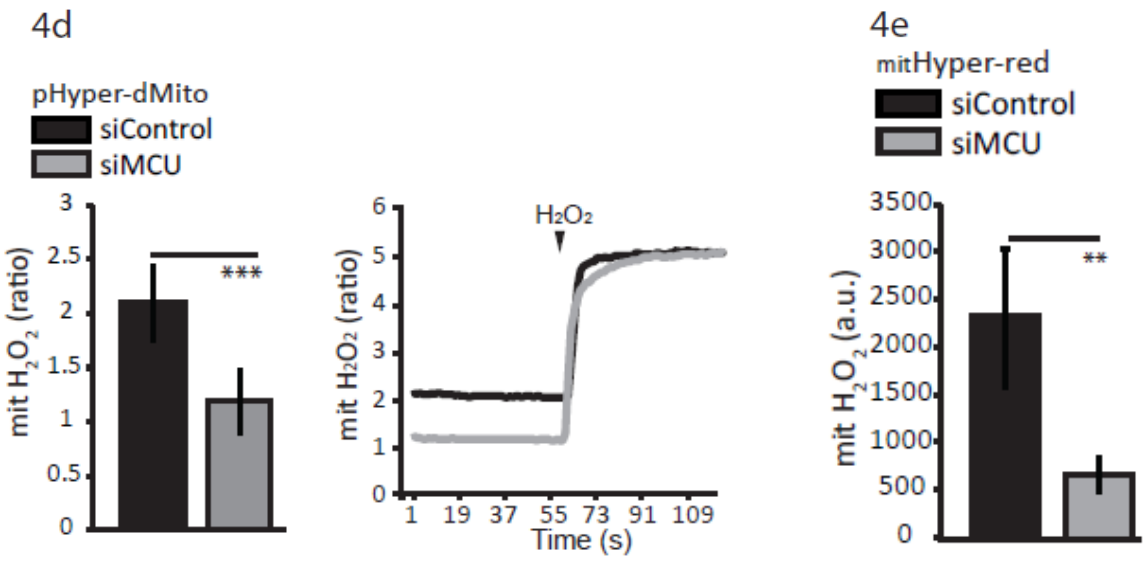

FIG.4d-e. **Mitochondrial H_2O_2 levels are critically blunted after MCU depletion.** Cells were transfected with siMCU or siControl, together with pHyper-dMito (Fig.4d) or HyPerRed probe (Fig.4e). 48 hours later H_2O_2 production was measured. H_2O_2 was added as a positive control (n=4, **p<0.01, ***p<0.001).

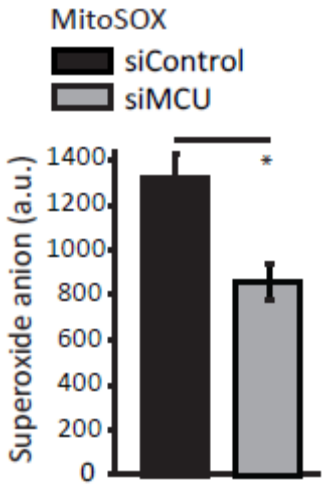

FIG.4f. **Mitochondrial superoxide levels are critically blunted after MCU silencing.** Cells were transfected with siMCU or siControl. 48 hours later cells

were loaded with the red dye MitoSOX^{TM} and superoxide anion levels were measured (n=6, *p<0.05).

MCU silencing alters the activity of Pyruvate Dehydrogenase (PDH) enzyme.

In agreement with the observation that MCU depletion causes an important drop in NAD(P)H production (Fig.3c), we aimed at understanding if any other critical metabolite could be affected by MCU silencing. Steady-state Mass Spectrometry (MS) analysis, performed by our collaborator Christian Frezza (MRC Cancer Unit - University of Cambridge) did not reveal significant changes either in metabolites involved in the TCA cycle activity, or in those involved in the glycolytic pathway in MCU-depleted cells, with the exception of a small, unexpected, increase in pyruvate level (Fig.5a).

We further investigated this finding, by measuring PDH phosphorylation level, as an indication of its activity. We observed that, after MCU silencing, PDH phosphorylation was unaffected (Fig.5b).

Since PDH is positively regulated by the Ca^{2+}-dependent Pyruvate Dehydrogenase Phosphatase (PDHP), we would have expected an accumulation of phospho-PDH (p-PDH) after MCU silencing, as already shown in different physiological models (Pan et al., 2013). However, PDH is also subjected to a negative control by the Pyruvate Dehydrogenase Kinase (PDK), which in turn is transcriptionally regulated by the hypoxia-inducible-factor-1α (HIF-1α). HIF-1α is a transcription factor that regulates a wide variety of cancer-related genes, involved in metastatic progression. Under normal O_2 concentration (i.e. about 20% [O_2]) HIF-1α is rapidly degraded by a mechanism involving the prolyl hydroxylase (PHD) and subsequent proteasome recruitment. However, under hypoxic conditions, common of most

solid tumors microenvironments, HIF-1α is stabilized. In MDA-MB-231 cells, HIF-1α was detected even in normoxic conditions (Fig.6a) and it was significantly accumulated upon O_2 deprivation (i.e. 2% [O_2], data not shown). Accordingly, we wanted to verify the effects of HIF-1α regulation on PDH enzyme. In order to stabilize HIF-1α and thus emphasize its physiological role, we incubated cells overnight in 2% [O_2]. Notably, in hypoxic conditions, we observed a significant decrease of p-PDH level after MCU depletion (Fig.5b). This data suggests a negative effect of MCU silencing on HIF-1α activity that might trigger PDH activation. A direct measure of PDH activity after MCU depletion further confirmed this result (Fig.5c).

The reason why MCU silencing potentiates PDH enzyme activity, and thus increase pyruvate level, without prompting the $_{mit}$OXPHOS activity, remains still an unsolved question, in the complicate metabolic scenery of this breast cancer model.

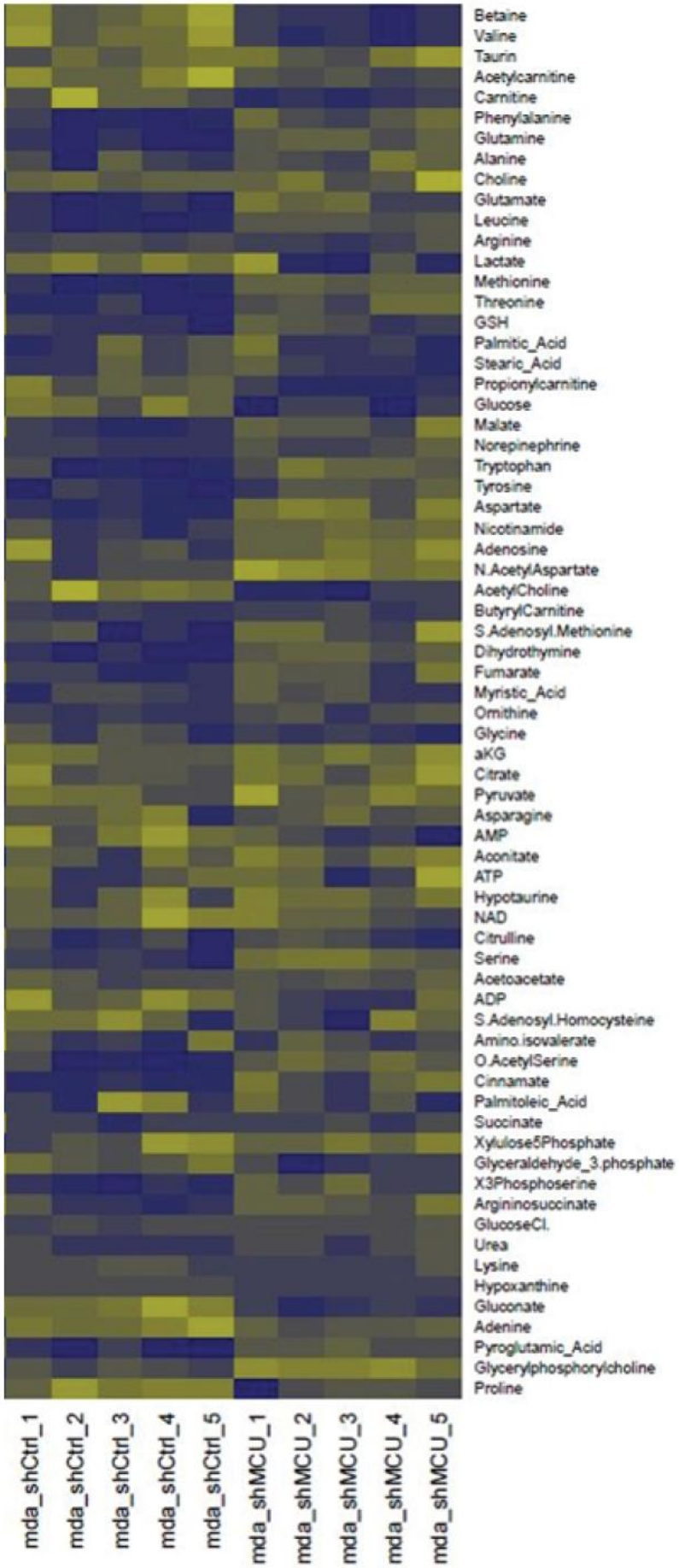
Betaine
Valine
Taurin
Acetylcarnitine
Carnitine
Phenylalanine
Glutamine
Alanine
Choline
Glutamate
Leucine
Arginine
Lactate
Methionine
Threonine
GSH
Palmitic_Acid
Stearic_Acid
Propionylcarnitine
Glucose
Malate
Norepinephrine
Tryptophan
Tyrosine
Aspartate
Nicotinamide
Adenosine
N.AcetylAspartate
AcetylCholine
ButyrylCarnitine
S.Adenosyl.Methionine
Dihydrothymine
Fumarate
Myristic_Acid
Ornithine
Glycine
aKG
Citrate
Pyruvate
Asparagine
AMP
Aconitate
ATP
Hypotaurine
NAD
Citrulline
Serine
Acetoacetate
ADP
S.Adenosyl.Homocysteine
Amino.isovalerate
O.AcetylSerine
Cinnamate
Palmitoleic_Acid
Succinate
Xylulose5Phosphate
Glyceraldehyde_3.phosphate
X3Phosphoserine
Argininosuccinate
GlucoseCl.
Urea
Lysine
Hypoxanthine
Gluconate
Adenine
Pyroglutamic_Acid
Glycerylphosphorylcholine
Proline
mda_shCtrl_1
mda_shCtrl_2
mda_shCtrl_3
mda_shCtrl_4
mda_shCtrl_5
mda_shMCU_1
mda_shMCU_2
mda_shMCU_3
mda_shMCU_4
mda_shMCU_5

FIG.5a. **MCU silencing does not compromise TCA or glycolysis-related metabolites.** Cells were infected with shMCU or shControl and Mass Spectrometry (MS) analysis was performed (n=5).

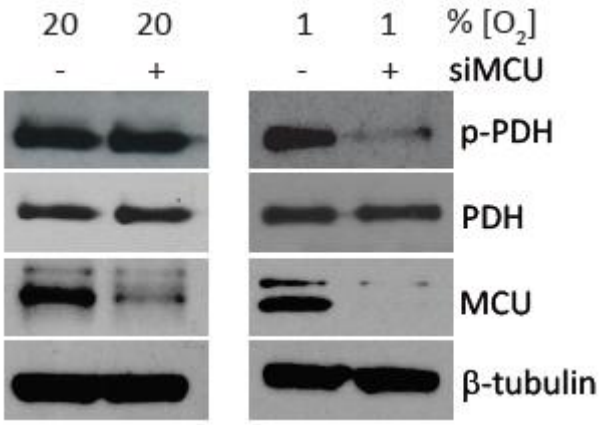

FIG.5b. **PDH phosphorylation is unaffected after MCU depletion in normoxic conditions, while it is decreased under hypoxia.** Cells were transfected with siMCU or siControl. After 48 hours p-PDH levels were detected by western blot.

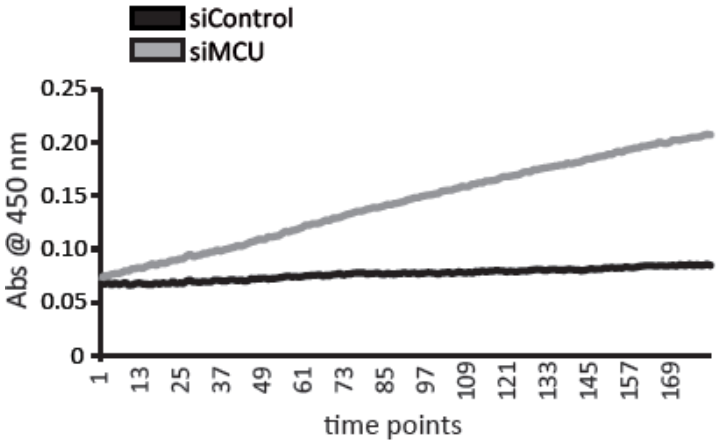

FIG.5c. **MCU silencing enhances PDH activity.** Cells were transfected with siMCU or siControl. After 48 hours PDH activity was measured (n=4).

MCU silencing strongly affects HIF-1α protein level.

The data reported above suggest that HIF-1α might play an important role in our model and deserves further investigation. HIF-1α regulates a large variety of target genes controlling the malignancy of several tumor types (Semenza, 2010a).

We wished to understand whether MCU controls HIF-1α activity in TNBC. MCU silencing caused a direct robust downregulation of HIF-1α protein (Fig. 6a). Aiming at understanding how siMCU induces HIF-1α depletion, we first investigated the most canonical pathway of HIF-1α protein degradation, via PHD activity and proteasome recruitment. We reasoned that, if siMCU enhanced HIF-1α protein degradation, proteasome inhibition should lead to accumulation of the hydroxylated form OH-HIF-1α (see Introduction, Fig. 2). Thus, we treated MDA-MB-231 cells with the proteasome inhibitor MG132 at different time points and monitored protein levels of both HIF-1α and OH-HIF-1α. Surprisingly, a significantly lower accumulation of OH-HIF-1α occurred in siMCU samples after MG132 treatment, compared to cell transfected with control siRNA (Fig.6b), thus suggesting that proteasome-mediated degradation is not responsible for siMCU-dependent HIF-1α depletion. Hence, an alternative mechanism should be involved. In order to confirm this hypothesis we thought to separate the effect of siMCU on HIF-1α protein levels from a putative role of MCU on HIF-1α transcription. For this purpose we overexpressed a plasmid encoding a HA-tagged, CMV-promoter driven, HIF-1α (HA- HIF-1α). Again, we inhibited the proteasome activity by MG132 treatments. Western blot analysis revealed small differences in HA tag levels between siMCU and control samples (Fig.6c), confirming that MCU silencing only partially controls HIF-1α protein stability.

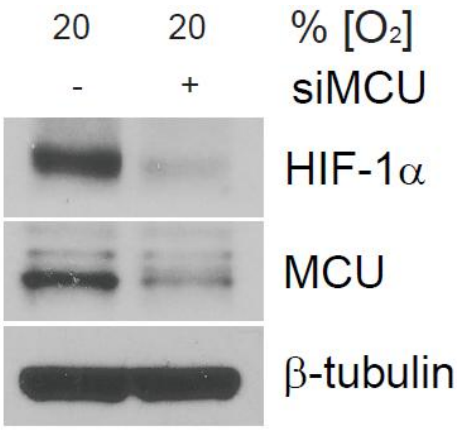

FIG.6a. HIF-1α levels are reduced after MCU silencing. Cells were transfected with siMCU or siControl. After 48 hours HIF-1α protein levels were measured by western blot.

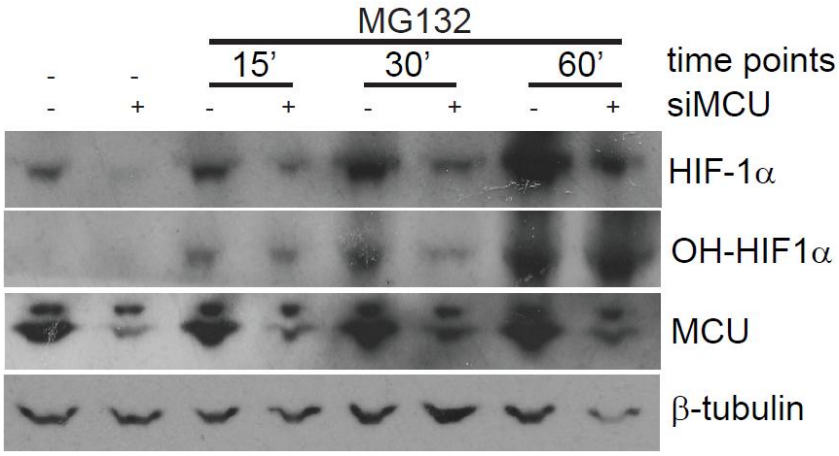

FIG.6b. **OH-HIF-1α levels are reduced after MCU silencing**. Cells were transfected with siMCU or siControl. 48 hours after transfection cells were treated with the proteasome inhibitor MG132. OH-HIF-1α protein levels were revealed by western blot.

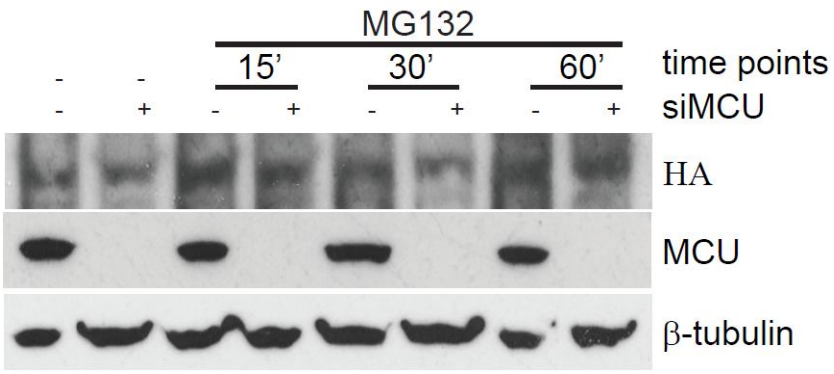

FIG.6c. **HIF-1α-HA levels are not significantly reduced after MCU silencing.** Cells were transduced with siMCU or siControl, together with retro-HIF-1α-HA. 48 hours later cells were treated with MG132 and HA tag levels were detected by western blot.

A possible alternative mechanism would be that MCU regulates HIF-1α transcription. Accordingly, measurements of HIF-1α mRNA levels demonstrated that siMCU strongly reduces HIF-1α gene expression, both in normoxic and in hypoxic conditions. Notably, also HIF-2α mRNA levels were significantly blunted by siMCU. In addition, selected HIF-target genes that, as expected, were upregulated in hypoxia, were also downregulated by siMCU (Fig.6d).

Hence, we aimed at identifying the key effectors triggering siMCU-mediated transcriptional downregulation on HIF-1α. We focused on ROS-mediated signalling as regulators of gene transcription. As expected, mitochondrial ROS depletion, by MitoTEMPO treatments, significantly blunted HIF-1α and HIF-1α -target genes mRNA expression (Fig. 6e).

Finally we wished to verify whether HIF-1α determines shMCU-mediated effects on cell migration. We observed that HIF-1α overexpression (both by wild type and by constitutively

active HIF-1α expression plasmids) is able to significantly rescue siMCU-mediated migration impairment (Fig.6f) demonstrating that HIF-1α is a crucial downstream effector of siMCU-induced block of migration.

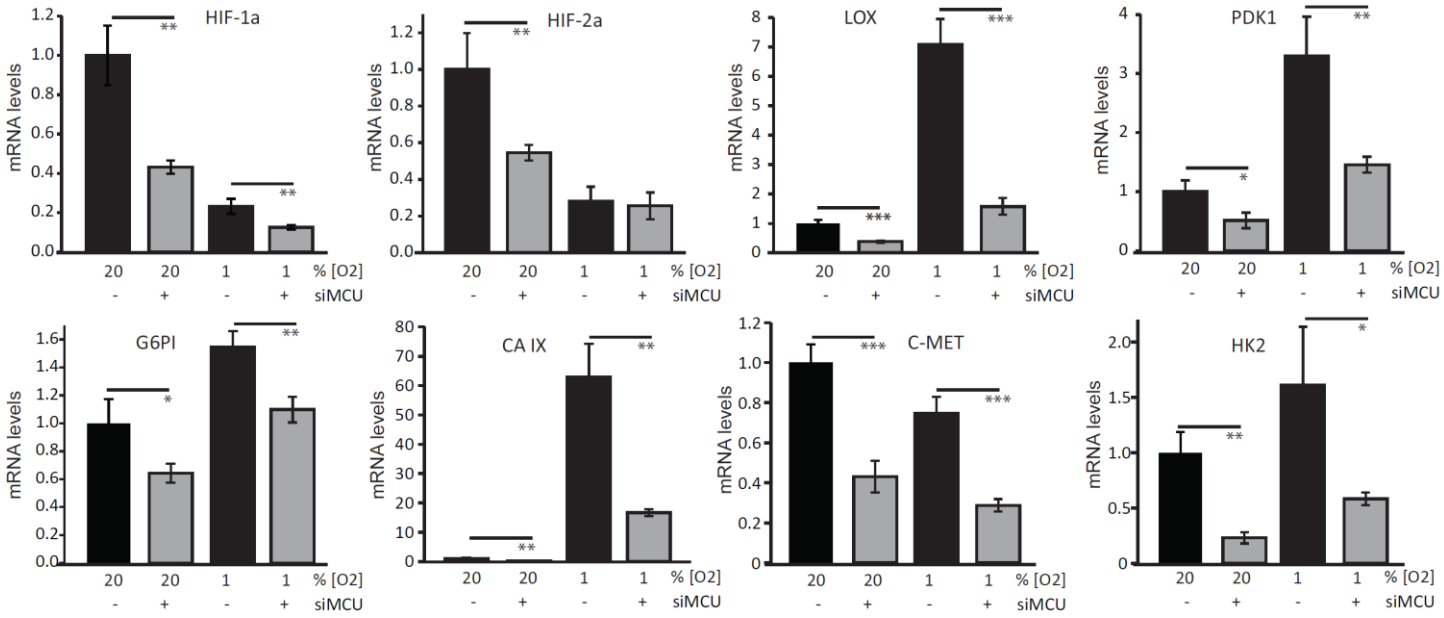

FIG.6d. **MCU silencing significantly reduces mRNA levels of HIF-1α and its regulated genes.** Cells were transfected with siMCU or siControl. mRNA expression of HIF-1α and HIF-1α regulated genes was measured by RealTime-PCR (n=3, *p<0.05, **p<0.01, ***p<0.001).

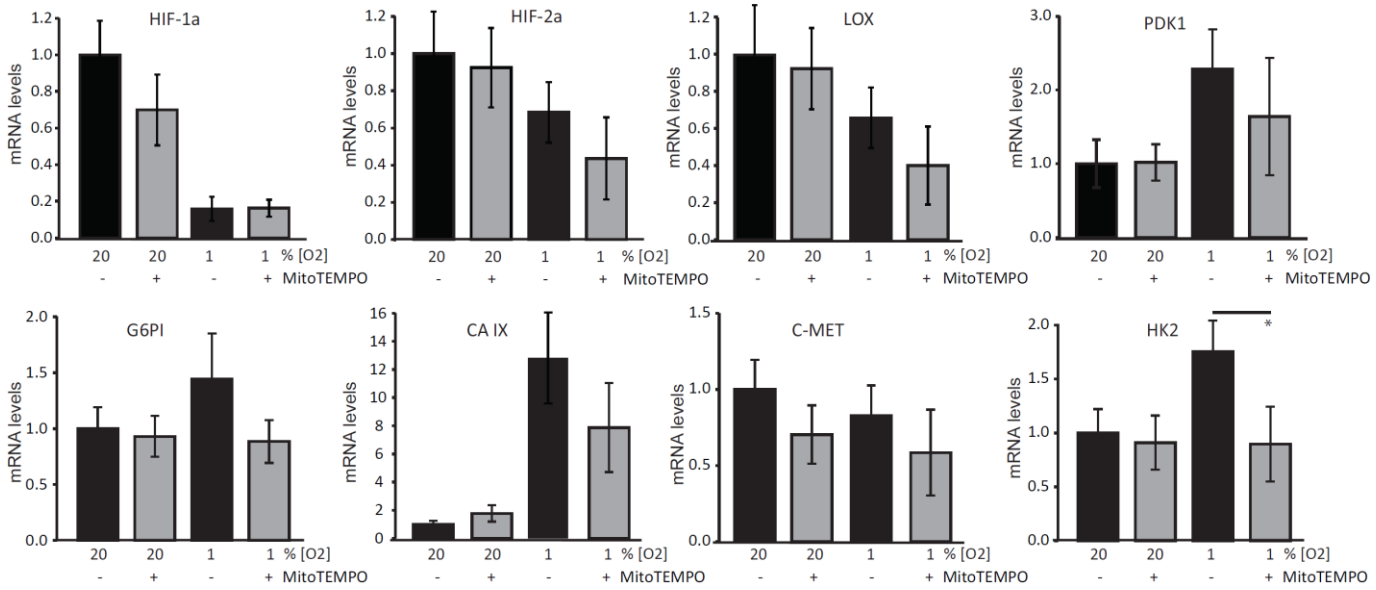

FIG.6e. **Antioxidant treatment reduces mRNA levels of HIF-1α and its regulated genes.** Cells were treated with MitoTEMPO for 48 hours. mRNA expression of HIF-1α and HIF-1α regulated genes was measured by RealTime-PCR (n=3, *p<0.05).

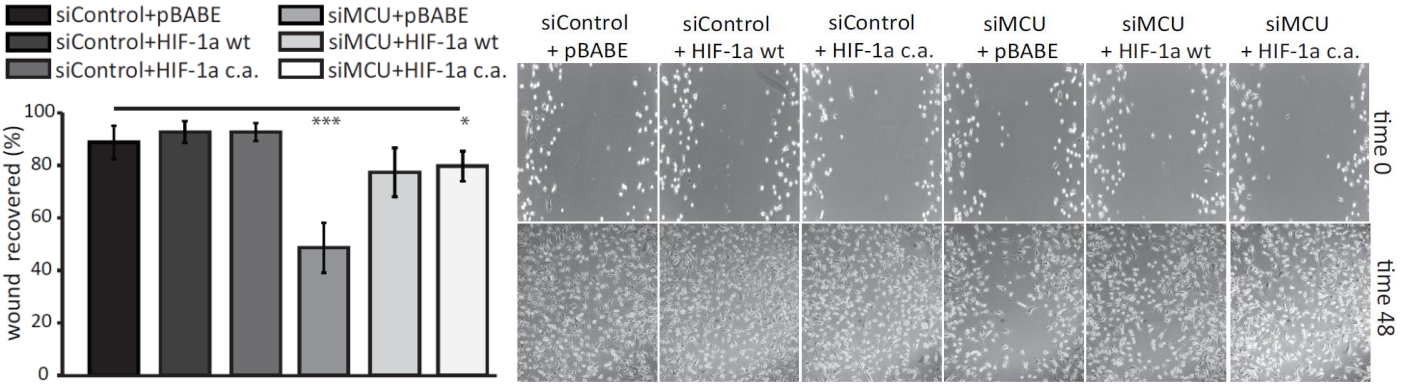

FIG.6f. **HIF-1α overexpression rescues siMCU-mediated migration impairment.** Cells were transfected with siMCU or siControl. HIF-1α (wt and c.a.) were overxpressed by retroviral infection (pBABE as control). The day after transduction cells were scratched (time point 0h). Cell migration into the wounded area was monitored at 48-hour time point and the recovered area was measured (n=3, *p<0.05, ***p<0.001).

DISCUSSION AND CONCLUSION

Using a triple negative breast cancer (TNBC) cell model we investigated the contribution of the mitochondrial Ca^{2+} to metastatic progression.

The molecular characterization of the Mitochondrial Calcium Uniporter (MCU) subunits (Baughman et al., 2011; De Stefani et al., 2011) prompted the interest in understanding new critical roles of Ca^{2+}_{mit} uptake in the pathophysiology of cancers.

It is widely recognized that the role of Ca^{2+} in the mitochondrial matrix goes far beyond the general stimulation of cellular energetics. In particular, the role of Ca^{2+}_{mit} accumulation in tumor cell survival and response to apoptotic stimuli has been widely investigated (Curry et al., 2013; Mallilankaraman et al., 2012b). In addition, in recent times the idea that mitochondrial Ca^{2+} signalling is required for cancer cell progression has been supported by the striking correlation between MCU gene overexpression and poor prognosis outcomes, in human breast cancer (Hall et al., 2014). At first sight this evidence may appear in contrast with the previous finding that a miRNA that specifically targets MCU is expressed in colon and prostate primary tumors (Marchi et al., 2013). However, it should be taken into account that cancer cells shall adapt and acquire pro-survival mechanisms during their metastatic progression, with the aim of developing an unrestrained proliferation. Accordingly, we hypothesized that, while in primary tumors low Ca^{2+}_{mit} loading should be preserved in order to avoid any apoptotic stimuli sensitization, in metastatic cells, which already escaped death and progress to a malignant phenotype, Ca^{2+}_{mit} transients might have different favourable roles. To verify this hypothesis, we first focused on two different breast cancer models derived from the MCF10 cell system, which allowed us to compare Ca^{2+}_{mit} uptake between pre-malignant (MCF10AT1kcl.2) and highly metastatic (MCF10CA1a.cl.1) cell lines. Upon

agonist stimulation, metastatic cells transiently accumulated much higher $[Ca^{2+}]_{mit}$ than the pre-malignant ones. We thus speculated that elevate Ca^{2+}_{mit} transients might be essential for metastatic progression, while being lethal for pre-malignant cells. In order to validate our hypothesis we chose three different TNBC metastatic cell lines (BT-549, MDA-MB-231, MDA-MB-468) and selectively knockdown MCU, thus significantly abolishing Ca^{2+}_{mit} uptake. We simultaneously monitored the capacity of those cells to migrate and recover a scratched area. Outstandingly, MCU suppression strongly reduced all three TNBC lines migration potential, without affecting cell proliferation or death, nor reverting the mesenchymal phenotype to epithelial traits. This finding was further supported by pharmacological inhibition of the MCU channel activity. For subsequent investigations, MDA-MB-231 cells were chosen. First, we verified MCU silencing effects on an additional fundamental metastatic feature: the surrounding matrix invasiveness. This competence is a critical hallmark of metastatic cells that mimics, *in vitro*, their potential to spread into distant tissues. Notably, MCU stable depletion affected the potential to invade the surrounding matrix that, in the long term, is sustained also by an impaired cell proliferation, as revealed by the clonogenic assay.

Our results highlight a new and intriguing role of mitochondrial Ca^{2+} in the regulation of metastatic cell migration and matrix invasiveness, which till now has been completely unexplored. The cellular events that underlie this process are still subject to intensive study and do not seem to involve mitochondrial membrane depolarization or mitochondrial OXPHOS activity suppression. Neverthless, we found a significant reduction in NAD(P)H/NAD ratio following MCU silencing, which might be explained by a general slowdown of the TCA functionality, considering that Ca^{2+} ions positively control the activity of three TCA cycle-related enzymes. On this basis, we considered, as possible consequence of MCU silencing, an impaired Reactive Oxygen Species (ROS) production. Indeed, ROS molecules have been

commonly accepted as critical triggers of metastatic progression, both *in vitro* and *in vivo* (Porporato et al., 2014), in agreement with the observation that, also in our model, antioxidant treatments (in particular the one selective for mitochondrial ROS scavenging, i.e. MitoTEMPO) result in migration impairment. ROS production was significantly blunted after siMCU, as suggested by an accurate oxidative-stress analysis, performed by means of four different mitochondria-targeted redox sensitive probes. Thus, the final outcome of MCU depletion signal appears to depend on alterations in the redox potential, which could in turn involve a large number of intracellular signalling cascades. However, our evidence reveals a smaller effect of ROS depletion on migration, compared to MCU knockdown. This observation suggests that ROS molecules only partially mediate siMCU effects on the metastatic progression, even if they certainly participate to this regulation. Thus, additional effectors, which deserve additional investigation, should partecipate to siMCU phenotype.

In order to further explore these findings, we took advantage of a steady-state MS analysis, looking for critical metabolic alterations following Ca^{2+}_{mit} depletion. Unexpectedly, in MCU silenced samples no significant changes in TCA cycle or glycolysis-related metabolites occured, with the only exception of a small increase in the pyruvate amount. These data, together with an enhanced Pyruvate Dehydrogenase Enzyme (PDH) activity, upon MCU silencing, left unanswered questions on possible metabolic adaptations arising from Ca^{2+}_{mit} reduction, in this complex metastatic model.

Our results prompted us to consider as final effector of MCU depletion the hypoxia-inducible-factor-1α (HIF-1α), one of the master regulators of metastasis, which is as well the main negative regulator of PDH activity. We obtained evidence of a critical and intriguing downregulation of HIF-1α transcription by MCU silencing, resulting from a novel proteasome-indipendent regulatory mechanism. The intracellular determinants of HIF-1α transcriptional regulation might include ROS as key signalling molecules.

On this line, our data demonstrate that ROS scavenging controls HIF-1α (and its regulated genes) mRNA expression, although at a lesser extent compared to siMCU.

Noteworthy, HIF-1α overexpression is completely able to rescue MCU silencing-induced migration impairment, suggesting that it represents the key final effector triggering siMCU-mediated phenotype.

MATERIALS AND METHODS

Cell cultures.

Five different cell lines were used to perform distinct experiments: MDA-MB-231, BT-549, MDA-MB-468, MCF10AT1k.cl2 and MCF10CA1a.cl1.

BT-549 and MDA-MB-468 cells were cultured in Dulbecco's modified Eagle's medium (DMEM) (cat# 41966-029 Life technologies), supplemented with 10% Fetal Bovine Serum (FBS) (cat# 10500-064, Life technologies).

MDA-MB-231 cells were cultured in DMEM/F12 medium (1:1) (cat# 31331-028, Life technologies), supplemented with 10% FBS (Life technologies).

MCF10AT1k.cl2 and MCF10CA1a.cl1 cells were cultured in DMEM/F12 freshly supplemented with 5% Horse Serum (HS), 10µg/ml Insulin, 20ng/ml EGF, 8.5ng/ml Cholera Toxin, 500ng/ml hydrocortisone.

All media were supplemented with 1% Penicillin G - Streptomycin Sulfate (cat# ECB3001, Euroclone) and 1% L-Glutammine (cat# ECB3000D, Euroclone).

Cells were maintained in culture at 37°C, with 5% CO_2. A subcultivation ratio of 1:6 to 1:10 was guaranteed.

Chemical compound treatments.

For KB-R7943 treatments (K4144, purchased by Sigma) cells were incubated for 48 hours with complete DMEM-10%FBS supplemented with 2 µM of drug (stock 20 mM in DMSO). Drug-containing medium must be changed every 24 hours with fresh one.

For the proteasome inhibitor MG132 treatments (#D00132451, Calbiochem) cells were incubated for 15', 30' and 1 hour with complete drug-containing medium, at a final concentration of 10 µM.

Transient transfections , infection and stable transduction.

Oligonucleotides (10 pmoles/cm^2) were transfected using a standard Lipofectamine® RNAiMAX Transfection Reagent (cat# 13778-150, Life technologies). To silence MCU a specific siRNA was designed:

siRNA-MCU:

nucleotides 899–917 of the corresponding mRNA (5'-GCCAGAGACAGACAAUACUtt-3' and 3'-ttCGGUCUCUGUCUGUUAUGA-5').

Adenovirus expressing mitochondrial mutated aequorin (AdCMVmAqMut) was constructed by Rutter et al. from plasmid mtAEQmut (Rizzuto et al., 1992) through the insertion of an EcoRI fragment into the multiple cloning site of pcDNA 3 (Invitrogen), and a correctly orientated *Kpn*I/*Xho*I fragment was inserted into vector pAdTrackCMV (Ainscow and Rutter, 2001).

The adenovirus expressing MCU-Flag was created (Raffaello et al., 2013) using the AdEasy strategy (Stratagene). Mouse MCU was cloned in the pAdTrack-CMV vector (Stratagene) using the following primers:

fw: 5'-GGTACCGCCACCATGGCGGCCGCCGCAGGTAG-3'

rv: 5'-CTCGAGTCACTTATCGTCGTCATCCTTGTAATCTTCCTTTTCTCCGATCTGTC-3'

The PCR fragment was cloned into KpnI and XhoI sites in pAdTrack-CMV. Subsequent steps were performed according to the manufacturer's instructions (Stratagene). Adenoviral vectors contain two distinct promoters that independently drive the expression of the gene of interest and of GFP. Therefore, mock plasmid expresses only GFP protein.

To create the constructs for MCU stable knock-down in MDA-MB-231, two interfering sequences were selected and cloned into pLKO.1-TRC Cloning vector, according to manifacturer's protocol (Addgene):

shRNA#1:

fw: 5’-CCGGGCAAGGAGTTTCTTTCTCTTTCTCGAGAAAGAGAAAGAAACTCCTTGCTTTTTG-3’

rv:5’-AATTCAAAAAGCAAGGAGTTTCTTTCTCTTTCTCGAGAAAGAGAAAGAAACTCCTTGC-3’

shRNA#2:

fw: 5’-CCGGTCAAAGGGCTTAGTGAATATTCTCGAGAATATTCACTAAGCCCTTTGATTTTTG-3’

rv: 5’- AATTCAAAAATCAAAGGGCTTAGTGAATATTCTCGAGAATATTCACTAAGCCCTTTGA-3’

Each contruct was controlled by sequencing and Western Blotting. We generated lentiviral particles from the simultaneous transfection of recombinant shuttle vectors (pCMV8.74 and pMD2.VSVG) and the two pLKO.1shRNAs, in packaging HEK293T cells.

HIF-1α overexpression was obtained by transducing MDA-MB-231 cells with retroviral vectors (for pCL and pBABE vectors, see plasmids list below). The efficiency of overexpression was controlled by Western Blotting.

For transient ROS-sensitive probes expression, DNA plasmids were transfected using LT1 reagent (cat# MIR 2300, Mirus).

Plasmids.

pLPCXmitGrx1-roGFP2 and HyperRed were a gift from I. Bogeski.

pHyPer-dMito was purchased by Evrogen (#FP942).

pCMV8.74 and pMD2.VSVG were gently provided by M. Montagner.

pLKO.1puro-NonTarget shRNA Control was purchased by Sigma (#SHC016V).

pLKO.1-TRC Cloning Vector (#8453), HA-HIF-1α-wt-pBABE (#19365), HA-HIF-1α-P402A/P564A (#19005) , pBABE-puro (#1764) and pCL (#12371) were obtained from Addgene.

Western Blotting and Antibodies.

To monitor endogenous and overexpressed protein regulation, cells were lysated in RIPA-buffer (150 mM NaCl, 50 mM Tris, 1 mM EGTA, 1% Triton X-100, 0.1%SDS) and after 30' of incubation on ice, 40 µg of total proteins were loaded according to BCA quantification. Proteins were separated by SDS-PAGE electrophoresis, in commercial 4-12% acrylamide gels (Life technologies) and transferred onto nitrocellulose membranes (Life technologies) by wet electrophoretic transfer. Blots were blocked 1 hr at RT with 5% non-fat dry milk (BioRad) in TBS (0.5M Trizma –Sigma, 1.5M NaCl) solution (0.01% Tween) and incubated at 4°C with primary antibodies. Secondary antibodies were incubated 1 hr at RT. Washes after antibody incubations were done on an orbital shaker, three times for 10'each, with TBS-0,01% tween.
We used the following antibodies: anti-MCU (1:1000, Sigma #HPA016480), anti-β-tubulin (1:7500, Santa Cruz #sc-9104), anti-HA (1:2000, Santa Cruz #sc-7392), anti-HIF1α (1:500, Becton Dickinson #610958), anti-hydroxy-HIF1α (1:1000, Cell Signaling #3434), anti-E-Cadherin (1:1000, Santa Cruz #sc-21791), anti-Vimentin (1:1000, Santa Cruz #sc-5565), anti-Twist (1:1000, Santa Cruz #sc-15393), anti-phospho-PDH (1:2000, Abcam #ab92696), anti-PDH (1:1000, Cell Signaling #2784).
Secondary, HRP-conjugated antibodies (1:5000) were purchased from BioRad.

Aequorin as a Ca^{2+} indicator.

Aequorin is a 21 KDa photoprotein isolated from jellyfish *Aequorea Victoria* which emits blue light in the presence of Ca^{2+}. The aequorin originally purified from the jellyfish is a mixture of different isoforms called "heterogeneous aequorin" (Shimomura, 1986). In its active form the photoprotein includes an apoprotein and a covalently bound prosthetic group, called coelenterazine. The apoprotein contains four helix-loop-helix "EF-hand" domains, three of which are Ca^{2+}-binding sites. These domains confer to the protein a particular globular structure forming the hydrophobic core cavity that accommodates the ligand

coelenterazine. When Ca^{2+} ions bind to the three high affinity EF-hand sites, coelenterazine is oxidized to coelenteramide, with a concomitant release of CO_2 and emission of light (Head et al. 2000). Although this reaction is irreversible, an active aequorin can be obtained *in vitro* by incubating the apoprotein with coelenterazine in the presence of oxygen and 2-mercaptoethanol. Reconstitution of an active aequorin (expressed recombinantly) can be obtained also in living cells by simple addition of coelenterazine into the medium. Coelenterazine is highly hydrophobic and has been shown to permeate cell membranes of various cell types. Different coelenterazine analogues have been synthetized and are now commercially available.

The possibility of using aequorin as Ca^{2+} indicator is based on the existence of a well-characterized relationship between the rate of photon emission and the free $[Ca^{2+}]$. The first method used to correlate the amount of photons emitted to the free $[Ca^{2+}]$ was that described by Allen and Blinks (Blinks, 1978). In the following years, this system was improved to achieve a simple algorithm that converts luminescence into $[Ca^{2+}]$ values. Under physiological conditions of pH, temperature and ionic strength, this relationship is more than quadratic in the range of $[Ca^{2+}]$ 10^{-5}-10^{-7} M. The presence of 3 Ca^{2+} binding sites in aequorin is responsible for the steep relationship between photon emission rate and free $[Ca^{2+}]$. The $[Ca^{2+}]$ can be calculated from the formula L/Lmax where L is the rate of photon emission at any instant during the experiment and Lmax is the maximal rate of photon emission at saturating $[Ca^{2+}]$. The rate of aequorin luminescence is independent of $[Ca^{2+}]$ at very high (>10^{-4} M) and very low $[Ca^{2+}]$ (< 10^{-7} M). However, as described below in more details, it is possible to expand the range of $[Ca^{2+}]$ that can be monitored with aequorin.

Although aequorin luminescence is not influenced either by K^+ or Mg^{2+} (which are the most abundant cations in the intracellular environment and thus the most likely source of interference in physiological experiments) both ions are competitive inhibitors of Ca^{2+}

activated luminescence.

pH was also shown to affect aequorin luminescence but at values below 7. Due to the characteristics described above, experiments with aequorin need to be done in well-controlled conditions of pH and ionic concentrations, notably of Mg^{2+}.

Recombinant aequorins.

Aequorin began to be widely used when the cDNA encoding the photoprotein was cloned, thus avoiding the purification of the native polypeptide and its microinjection. Moreover, the cloning of aequorin gene opened the way to recombinant expression and thus has largely expanded the applications of this tool for investigating Ca^{2+} handling in living cells. In particular, recombinant aequorin can be expressed not only in the cytoplasm, but also in specific intracellular compartments by including specific targeting sequences in the engineered cDNAs (Hartl et al., 1989). Extensive manipulations of the N-terminal of aequorin have been shown not to alter the chemiluminescence properties of the photoprotein and its Ca^{2+} affinity. On the other hand, even marginal alterations of the C-terminal either abolish luminescence or drastically increase Ca^{2+} independent photon emission. For these reasons, all targeted aequorins synthesized in our laboratory include modifications of the photoprotein N-terminal. Three targeting strategies have been adopted:

1. Inclusion of a minimal targeting signal sequence to the photoprotein cDNA. This strategy was initially used to design the mitochondrial aequorin and was followed also to synthesize an aequorin localized in the nucleus and in the lumen of the Golgi apparatus.

2. Fusion of the cDNA encoding aequorin to that of a resident protein of the compartments of interest. This approach has been used to engineer aequorins localized in the sarcoplasmic reticulum (SR), in the nucleoplasm and cytoplasm (shuttling between the two compartments depending on the concentration of steroid hormones), on the cytoplasmic surface of the

endoplasmic reticulum (ER) and Golgi and in the subplasmalemma cytoplasmic rim.

3. Addition to the aequorin cDNA of sequences that code for polypeptides that bind to endogenous proteins. This strategy was adopted to localize aequorin in the ER lumen.

The construct used in our experiments is the mutated isoform of mitochondrial targeted aequorin (Brini, 2008): mtAEQmut. It was generated to measure the [Ca^{2+}] of the mitochondrial matrix of various cell types. This construct includes the targeting presequence of subunit VIII of human cytochrome c oxidase fused to the aequorin cDNA. To expand the range of Ca^{2+} sensitivity that can be monitored the photoprotein was also mutated (Asp119>Ala). This point mutation affects specifically the second EF hand motive of wild type aequorin. The affinity for Ca^{2+} of this mutated aequorin (mtAEQmut) is about 20 fold lower than that of the wild type.

Luminescence detection.

The aequorin detection system is derived from that described by Cobbold and Lee (Cobbold and Bourne, 1984) and is based on the use of a low noise photomultiplier placed in close proximity (2-3 mm) with aequorin expressing cells. Cells are seeded on 13-mm coverslips and put into a perfusion chamber. The volume of the chamber is kept to a minimum (about 200 µl). Cells are continuously perfused via peristaltic pump with KRB saline solution, thermostated via a water bath at 37°C.

The photomultiplier (Hamamatsu H7301) is kept into a dark box. The output of the amplifier-discriminator is captured by C8855-01-photoncounting board in an IBM compatible microcomputer and stored for further analysis.

Experimental procedures for Ca^{2+} measurments.

Cells were seeded onto 13 mm glass coverslips and allowed to grow to 50% confluence. The

day before measuring, cells were infected with Adeno-mtAEQmut virus (as previously described (Ainscow and Rutter, 2001) together with the indicated siRNA or plasmid.

The following day, coverslips with cells were incubated with 5 μM coelenterazine for 2 hours in KRB saline supplemented with 1mM $CaCl_2$, and then transferred to the perfusion chamber. All aequorin measurements were carried out in KRB saline solution. Agonists and other drugs were added to the same solution. The agonist stimuli used for maximal stimulation were: 100 μM histamine or 100 μM ATP, depending on the cell type.

The experiments were terminated by lysing cells with 100 μM digitonin in a hypotonic Ca^{2+}-rich solution (10 mM $CaCl_2$ in H2O), thus discharging the unbound aequorin pool. The light signal was collected and calibrated into free [Ca^{2+}] values by an algorithm based on the Ca^{2+} response curve of aequorin at physiological conditions of pH, [Mg^{2+}] and ionic strength, as previously described.

Measurement of Mitochondrial Membrane Potential.

The measurement of mitochondrial membrane potential is based on the distribution of the mitochondrion-selective lipofilic cation ”tetramethyl rhodamine methyl ester” dye (TMRM, Life Technologies). It is fluorescent and membrane permeable and its distribution into intracellular compartments is triggered by electrochemical gradients. Hence, at low concentrations, its accumulation into mitochondria was shown to be driven by mitochondrial membrane potential (almost -180mV). In order to promote the correct distribution of the probe, cells were loaded with the dye-solution at very low concentration (20 nM). Changes in mitochondrial membrane potential cause a redistribution of the dye between mitochondria and cytoplasmatic environment. Cells were loaded with TMRM stock solution (in KRB saline solution) for 20’ at 37°C. The probe was excited at 560 nm and the emission light was recorded in the 590-650 nm range.

Images were taken every 10 s with a fixed 200 ms exposure time. FCCP (carbonyl cyanide p-trifluoromethoxyphenylhydrazone, 10 µM), an uncoupler of oxidative phosphorylation, was added after 12 acquisitions to completely collapse the electrical gradient established by the respiratory chain (ΔΨ). Data are expressed as difference between the TMRM fluorescence before and after FCCP depolarization. Confocal laser microscope (Zeiss Axiovert 200, objective PlanFluar 40X/1.3) was used in TMRM experiments.

ROS production measurements.

To determine mitochondrial superoxide levels cells were labeled with 2 mM MitoSOX (Life Technologies) for 15‘ at 37°C. MitoSOX™ Red reagent is a novel fluorogenic dye specifically targeted to mitochondria in live cells. Oxidation of MitoSOX™ Red reagent by superoxide produces red fluorescence, which can be recorded with Absorption/emission maxima at ~510/580 nm. Maximal ROS production was induced with 10 mM Antimycin-A (Sigma) as a positive control.

In order to measure only mitochondrial Superoxide production and avoid any aspecific intracellular accumulation, we performed these measurements microscopically, and analyzed images by ImageJ software.

To determine hydrogen peroxide levels cells were transfected with different probe-expressing plasmids (HyperRed (Ermakova et al., 2014), pLPCXmitGrx1-roGFP2 and pHyPer-dMito) together with shMCU plasmid.

Cells were imaged in Ringer’s buffer solution 48 hours following plasmids transfection, using Cell Observer High Speed (Zeiss) microscope equipped with 40x oil Fluar (N.A. 1.3) or 100x oil alpha Plan-Fluar (N.A. 1.45) objective, CFP (Semrock HC) and YFP (Zeiss 46HE) singleband filters, 420 and 505 nm LED’s (Colibri, Zeiss) and an Evolve 512 EMCCD camera (Photometrics). Images were acquired every 5 s for a total of 50 s. Maximal ROS production

was induced with 10 mM H_2O_2 as a positive control. To calculate fluorescence ratios background intensity was subtracted and images were corrected for linear crosstalk. pHyPer-dMito and pLPCXmitGrx1-roGFP2 ratios were calculated by AxioVision software (Zeiss) and analyzed in Excel (Microsoft). HyperRed fluorescence was analized by ImageJ software. Statistical significance was determined using two-sided unpaired student's t-test.

Pyruvate Dehydrogenase enzyme activity.

PDH activity was measured using the PDH enzyme activity microplate assay kit (Abcam #ab109902).

Cytofluorimetric Analyses.

Cytofluorimetric analyses were utilized to analyze cell cycle and cell death induction with the use of Annexin V-FITC (Roche) and propidium iodide (Sigma) probes.

Oxygen Consumption Rate Experiments.

Mitochondrial respiration was followed in a kinetic mode by measuring the oxygen consumption rate (OCR) of cell monolayers with XF^e Extracellular Flux Analyzer (Seahorse Bioscience).

Wound healing migration assay.

For wound healing assays, cells were seeded and transfected at low confluency (30%) in 6-well plates, in complete medium. After 8 hours, cells were starved in medium without serum, for 24 hours. The day after, cell monolayers were scraped with a P200 tip, vertically held, to obtain a wound in each well; the medium was replaced with fresh one. Picture of

migrating cells were taken at the indicated time point (time 0 as reference). A free software tool called "TScratch" (www.chaton.ethz.ch/software) was used for automated images analysis.

Clonogenic assay.

To evaluate clonogenic potential, cells were counted (Scepter™ 2.0 Cell Counter) and seeded at very low density (10^3/well) into 6-well plates. After 7 days colonies were counted. Only colonies made of ≥ 30 cells were included in the quantification.

Sheroids formation assay.

We put $5*10^3$ cells/well in each well, of a 96-well plate, containing 100 µl Agar 1.5%. The plate was left for 72h in the incubator at 37°C. We put 300 µl of Collagen mix solution (L-Glutamine 1.66mM, FBS 10%, $NaHO_3$ 0.213%, Pen/Strep 1%, Collagen 2mg/ml, EMEM) per well, in a 24-well plate and waited until it got solid. We harvested spheroids grown into the 96-well plate with a 200 µl pipette (with cut tips). Spheroids were put in the Collagen mix solution and seeded in the 24-well plate containing the Collagen Mix (5 spheroids/400 µl/ well). After it got solid, 1 ml /well of complete medium was added. We cultivated cells for 3 days and took pictures every day.

Images were analyzed by Fiji ImageJ software, by calculating the area of the spheroid cluster (time 0 as reference).

RNA extraction, reverse transcription, and quantitative realtime PCR.

At least three samples were prepared for each condition. Total RNA was extracted from $2*10^6$ MDA-MB-231 cells using the SV Total RNA Isolation Kit (Promega) following the manufacturer's instructions. The RNA was quantified with an Eppendorf Bio photometer

Plus. From 400 nmol of total RNA of each sample, complementary DNA was generated with a cDNA synthesis kit (SuperScript II, Invitrogen) and analysed by real-time PCR using the SYBR green chemistry (Bio-Rad). The primers were designed and analysed with Primer3 (Rozen and Skaletsky, 2000). Real-time PCR standard curves were constructed by using serial dilution of cDNAs of the analysed samples, using at least four dilution points and the efficiency of all primer sets was between 98 and 102%. The housekeeping genes HPRT-1 and GAPDH were used as an internal control for cDNA quantification and normalization of the amplified products. Real-time PCR primer sequences were as follows:

HIF-1α:

FW: TGTACCCTAACTAGCCGAGGAA

RV: AATCAGCACCAAGCAGGTCATA

HIF-2α:

FW: AATGCAGTACCCAGACGGATTT

RV: ATGTTTGTCATGGCACTGAAGC

LOX:

FW: TCAGATTTCTTACCCAGCCGAC

RV: TTGGCATCAAGCAGGTCATAGT

PDK1:

FW: AATGCAAAATCACCAGGACAGC

RV: ATTACCCAGCGTGACATGAACT

G6PI:

FW: TTACTCCAAGAACCTGGTGACG

RV: CTACCAGGATGGGTGTGTTTGA

CA-IX:

FW: TGGCTGCTGGTGACATCCTA

RV: TTGGTTCCCCTTCTGTGCTG

C-MET:

FW: AGCAATGGGGAGTGTAAAGAGG

RV: GCACCAAGGAAAATGTGATGCT

HK2:

FW: GTGCCCGCCAGAAGACATTA

RV: TGCTCAGACCTCGCTCCATT

HPRT-1:

FW: TGACACTGGCAAAACAATGCA

RV: GGTCCTTTTCACCAGCAAGCT

GAPDH:

FW: GATTCCACCCATGGCAAATTCC

RV: CCCCACTTGATTTTGGAGGGAT

BIBLIOGRAPHY

Ainscow, E.K., and Rutter, G.A. (2001). Mitochondrial priming modifies Ca2+ oscillations and insulin secretion in pancreatic islets. Biochem J *353*, 175-180.

Barnett, P., Arnold, R.S., Mezencev, R., Chung, L.W., Zayzafoon, M., and Odero-Marah, V. (2011). Snail-mediated regulation of reactive oxygen species in ARCaP human prostate cancer cells. Biochem Biophys Res Commun *404*, 34-39.

Basso, E., Fante, L., Fowlkes, J., Petronilli, V., Forte, M.A., and Bernardi, P. (2005). Properties of the permeability transition pore in mitochondria devoid of Cyclophilin D. J Biol Chem *280*, 18558-18561.

Baughman, J.M., Perocchi, F., Girgis, H.S., Plovanich, M., Belcher-Timme, C.A., Sancak, Y., Bao, X.R., Strittmatter, L., Goldberger, O., Bogorad, R.L.*, et al.* (2011). Integrative genomics identifies MCU as an essential component of the mitochondrial calcium uniporter. Nature *476*, 341-345.

Baysal, B.E., Ferrell, R.E., Willett-Brozick, J.E., Lawrence, E.C., Myssiorek, D., Bosch, A., van der Mey, A., Taschner, P.E., Rubinstein, W.S., Myers, E.N.*, et al.* (2000). Mutations in SDHD, a mitochondrial complex II gene, in hereditary paraganglioma. Science *287*, 848-851.

Belousov, V.V., Fradkov, A.F., Lukyanov, K.A., Staroverov, D.B., Shakhbazov, K.S., Terskikh, A.V., and Lukyanov, S. (2006). Genetically encoded fluorescent indicator for intracellular hydrogen peroxide. Nat Methods *3*, 281-286.

Ben Mahdi, M.H., Andrieu, V., and Pasquier, C. (2000). Focal adhesion kinase regulation by oxidative stress in different cell types. IUBMB Life *50*, 291-299.

Blacker, T.S., Mann, Z.F., Gale, J.E., Ziegler, M., Bain, A.J., Szabadkai, G., and Duchen, M.R. (2014). Separating NADH and NADPH fluorescence in live cells and tissues using FLIM. Nat Commun *5*, 3936.

Blinks, J.R. (1978). Applications of calcium-sensitive photoproteins in experimental biology. Photochem Photobiol *27*, 423-432.

Boivin, B., Yang, M., and Tonks, N.K. (2010). Targeting the reversibly oxidized protein tyrosine phosphatase superfamily. Sci Signal *3*, pl2.

Brini, M. (2008). Calcium-sensitive photoproteins. Methods *46*, 160-166.

Cannito, S., Novo, E., Compagnone, A., Valfre di Bonzo, L., Busletta, C., Zamara, E., Paternostro, C., Povero, D., Bandino, A., Bozzo, F.*, et al.* (2008). Redox mechanisms switch on hypoxia-dependent epithelial-mesenchymal transition in cancer cells. Carcinogenesis *29*, 2267-2278.

Cardenas, C., Miller, R.A., Smith, I., Bui, T., Molgo, J., Muller, M., Vais, H., Cheung, K.H., Yang, J., Parker, I.*, et al.* (2010). Essential regulation of cell bioenergetics by constitutive InsP3 receptor Ca2+ transfer to mitochondria. Cell *142*, 270-283.

Cobbold, P.H., and Bourne, P.K. (1984). Aequorin measurements of free calcium in single heart cells. Nature *312*, 444-446.

Criollo, A., Maiuri, M.C., Tasdemir, E., Vitale, I., Fiebig, A.A., Andrews, D., Molgo, J., Diaz, J., Lavandero, S., Harper, F.*, et al.* (2007). Regulation of autophagy by the inositol trisphosphate receptor. Cell Death Differ *14*, 1029-1039.

Csordas, G., Golenar, T., Seifert, E.L., Kamer, K.J., Sancak, Y., Perocchi, F., Moffat, C., Weaver, D., de la Fuente Perez, S., Bogorad, R.*, et al.* (2013). MICU1 controls both the threshold and cooperative activation of the mitochondrial Ca(2)(+) uniporter. Cell Metab *17*, 976-987.

Curry, M.C., Peters, A.A., Kenny, P.A., Roberts-Thomson, S.J., and Monteith, G.R. (2013). Mitochondrial calcium uniporter silencing potentiates caspase-independent cell death in MDA-MB-231 breast cancer cells. Biochem Biophys Res Commun *434*, 695-700.

Davies, K.J. (1995). Oxidative stress: the paradox of aerobic life. Biochem Soc Symp *61*, 1-31.

Davies, M.J. (2003). Singlet oxygen-mediated damage to proteins and its consequences. Biochem Biophys Res Commun *305*, 761-770.

De Stefani, D., Raffaello, A., Teardo, E., Szabo, I., and Rizzuto, R. (2011). A forty-kilodalton protein of the inner membrane is the mitochondrial calcium uniporter. Nature *476*, 336-340.

den Hertog, J., Ostman, A., and Bohmer, F.D. (2008). Protein tyrosine phosphatases: regulatory mechanisms. FEBS J *275*, 831-847.

Disatnik, M.H., and Rando, T.A. (1999). Integrin-mediated muscle cell spreading. The role of protein kinase c in outside-in and inside-out signaling and evidence of integrin cross-talk. J Biol Chem *274*, 32486-32492.

Droge, W. (2002). Free radicals in the physiological control of cell function. Physiol Rev *82*, 47-95.

Duarte, J.M., Schuck, P.F., Wenk, G.L., and Ferreira, G.C. (2014). Metabolic disturbances in diseases with neurological involvement. Aging Dis *5*, 238-255.

Duchen, M.R. (2004). Roles of mitochondria in health and disease. Diabetes *53 Suppl 1*, S96-102.

Elias, A.D. (2010). Triple-negative breast cancer: a short review. Am J Clin Oncol *33*, 637-645.

Ermakova, Y.G., Bilan, D.S., Matlashov, M.E., Mishina, N.M., Markvicheva, K.N., Subach, O.M., Subach, F.V., Bogeski, I., Hoth, M., Enikolopov, G.*, et al.* (2014). Red fluorescent genetically encoded indicator for intracellular hydrogen peroxide. Nat Commun *5*, 5222.

Fagan, J.B., and Racker, E. (1978). Determinants of glycolytic rate in normal and transformed chick embryo fibroblasts. Cancer Res *38*, 749-758.

Fang, M., Shen, Z., Huang, S., Zhao, L., Chen, S., Mak, T.W., and Wang, X. (2010). The ER UDPase ENTPD5 promotes protein N-glycosylation, the Warburg effect, and proliferation in the PTEN pathway. Cell *143*, 711-724.

Felton, V.M., Borok, Z., and Willis, B.C. (2009). N-acetylcysteine inhibits alveolar epithelial-mesenchymal transition. Am J Physiol Lung Cell Mol Physiol *297*, L805-812.

Fritz, V., and Fajas, L. (2010). Metabolism and proliferation share common regulatory pathways in cancer cells. Oncogene *29*, 4369-4377.

Gaude, E., and Frezza, C. (2014). Defects in mitochondrial metabolism and cancer. Cancer Metab *2*, 10.

Giannoni, E., Parri, M., and Chiarugi, P. (2012). EMT and oxidative stress: a bidirectional interplay affecting tumor malignancy. Antioxid Redox Signal *16*, 1248-1263.

Giorgi, C., Romagnoli, A., Pinton, P., and Rizzuto, R. (2008). Ca2+ signaling, mitochondria and cell death. Curr Mol Med *8*, 119-130.

Glancy, B., and Balaban, R.S. (2012). Role of mitochondrial Ca2+ in the regulation of cellular energetics. Biochemistry *51*, 2959-2973.

Gottlieb, E., and Tomlinson, I.P. (2005). Mitochondrial tumour suppressors: a genetic and biochemical update. Nat Rev Cancer *5*, 857-866.

Gutscher, M., Pauleau, A.L., Marty, L., Brach, T., Wabnitz, G.H., Samstag, Y., Meyer, A.J., and Dick, T.P. (2008). Real-time imaging of the intracellular glutathione redox potential. Nat Methods *5*, 553-559.

Hall, D.D., Wu, Y., Domann, F.E., Spitz, D.R., and Anderson, M.E. (2014). Mitochondrial calcium uniporter activity is dispensable for MDA-MB-231 breast carcinoma cell survival. PLoS One *9*, e96866.

Hanahan, D., and Weinberg, R.A. (2011). Hallmarks of cancer: the next generation. Cell *144*, 646-674.

Harris, A.L. (2002). Hypoxia--a key regulatory factor in tumour growth. Nat Rev Cancer *2*, 38-47.

Hartl, F.U., Pfanner, N., Nicholson, D.W., and Neupert, W. (1989). Mitochondrial protein import. Biochim Biophys Acta *988*, 1-45.

Hoyer-Hansen, M., and Jaattela, M. (2007). Connecting endoplasmic reticulum stress to autophagy by unfolded protein response and calcium. Cell Death Differ *14*, 1576-1582.

Hsu, P.P., and Sabatini, D.M. (2008). Cancer cell metabolism: Warburg and beyond. Cell *134*, 703-707.

Hu, C.T., Wu, J.R., Cheng, C.C., Wang, S., Wang, H.T., Lee, M.C., Wang, L.J., Pan, S.M., Chang, T.Y., and Wu, W.S. (2011). Reactive oxygen species-mediated PKC and integrin signaling promotes tumor progression of human hepatoma HepG2. Clin Exp Metastasis *28*, 851-863.

Hurd, T.R., DeGennaro, M., and Lehmann, R. (2012). Redox regulation of cell migration and adhesion. Trends Cell Biol *22*, 107-115.

Jouaville, L.S., Pinton, P., Bastianutto, C., Rutter, G.A., and Rizzuto, R. (1999). Regulation of mitochondrial ATP synthesis by calcium: evidence for a long-term metabolic priming. Proc Natl Acad Sci U S A *96*, 13807-13812.

Kondoh, H., Lleonart, M.E., Bernard, D., and Gil, J. (2007). Protection from oxidative stress by enhanced glycolysis; a possible mechanism of cellular immortalization. Histol Histopathol *22*, 85-90.

Koppenol, W.H., Bounds, P.L., and Dang, C.V. (2011). Otto Warburg's contributions to current concepts of cancer metabolism. Nat Rev Cancer *11*, 325-337.

Lasorsa, F.M., Pinton, P., Palmieri, L., Fiermonte, G., Rizzuto, R., and Palmieri, F. (2003). Recombinant expression of the Ca(2+)-sensitive aspartate/glutamate carrier increases mitochondrial ATP production in agonist-stimulated Chinese hamster ovary cells. J Biol Chem *278*, 38686-38692.

Lee, E.K., Jeon, W.K., Chae, M.Y., Hong, H.Y., Lee, Y.S., Kim, J.H., Kwon, J.Y., Kim, B.C., and Park, S.H. (2010). Decreased expression of glutaredoxin 1 is required for transforming growth factor-beta1-mediated epithelial-mesenchymal transition of EpRas mammary epithelial cells. Biochem Biophys Res Commun *391*, 1021-1027.

Levine, A.J., and Puzio-Kuter, A.M. (2010). The control of the metabolic switch in cancers by oncogenes and tumor suppressor genes. Science *330*, 1340-1344.

Mallilankaraman, K., Cardenas, C., Doonan, P.J., Chandramoorthy, H.C., Irrinki, K.M., Golenar, T., Csordas, G., Madireddi, P., Yang, J., Muller, M.*, et al.* (2012a). MCUR1 is an essential component of mitochondrial Ca2+ uptake that regulates cellular metabolism. Nat Cell Biol *14*, 1336-1343.

Mallilankaraman, K., Doonan, P., Cardenas, C., Chandramoorthy, H.C., Muller, M., Miller, R., Hoffman, N.E., Gandhirajan, R.K., Molgo, J., Birnbaum, M.J.*, et al.* (2012b). MICU1 is an essential gatekeeper for MCU-mediated mitochondrial Ca(2+) uptake that regulates cell survival. Cell *151*, 630-644.

Mannella, C.A. (2006). Structure and dynamics of the mitochondrial inner membrane cristae. Biochim Biophys Acta *1763*, 542-548.

Marchi, S., Lupini, L., Patergnani, S., Rimessi, A., Missiroli, S., Bonora, M., Bononi, A., Corra, F., Giorgi, C., De Marchi, E.*, et al.* (2013). Downregulation of the mitochondrial calcium uniporter by cancer-related miR-25. Curr Biol *23*, 58-63.

McCormack, J.G., Halestrap, A.P., and Denton, R.M. (1990). Role of calcium ions in regulation of mammalian intramitochondrial metabolism. Physiol Rev *70*, 391-425.

Mitchell, P. (1966). Chemiosmotic coupling in oxidative and photosynthetic phosphorylation. Biol Rev Camb Philos Soc *41*, 445-502.

Nishikawa, M. (2008). Reactive oxygen species in tumor metastasis. Cancer Lett *266*, 53-59.

Nobes, C.D., and Hall, A. (1999). Rho GTPases control polarity, protrusion, and adhesion during cell movement. J Cell Biol *144*, 1235-1244.

Nordberg, J., and Arner, E.S. (2001). Reactive oxygen species, antioxidants, and the mammalian thioredoxin system. Free Radic Biol Med *31*, 1287-1312.

Owens, K.M., Kulawiec, M., Desouki, M.M., Vanniarajan, A., and Singh, K.K. (2011). Impaired OXPHOS complex III in breast cancer. PLoS One *6*, e23846.

Pagliarini, D.J., Calvo, S.E., Chang, B., Sheth, S.A., Vafai, S.B., Ong, S.E., Walford, G.A., Sugiana, C., Boneh, A., Chen, W.K.*, et al.* (2008). A mitochondrial protein compendium elucidates complex I disease biology. Cell *134*, 112-123.

Pan, X., Liu, J., Nguyen, T., Liu, C., Sun, J., Teng, Y., Fergusson, M.M., Rovira, II, Allen, M., Springer, D.A.*, et al.* (2013). The physiological role of mitochondrial calcium revealed by mice lacking the mitochondrial calcium uniporter. Nat Cell Biol *15*, 1464-1472.

Patron, M., Checchetto, V., Raffaello, A., Teardo, E., Vecellio Reane, D., Mantoan, M., Granatiero, V., Szabo, I., De Stefani, D., and Rizzuto, R. (2014). MICU1 and MICU2 finely tune the mitochondrial Ca2+ uniporter by exerting opposite effects on MCU activity. Mol Cell *53*, 726-737.

Paupe, V., Prudent, J., Dassa, E.P., Rendon, O.Z., and Shoubridge, E.A. (2015). CCDC90A (MCUR1) Is a Cytochrome c Oxidase Assembly Factor and Not a Regulator of the Mitochondrial Calcium Uniporter. Cell Metab *21*, 109-116.

Perocchi, F., Gohil, V.M., Girgis, H.S., Bao, X.R., McCombs, J.E., Palmer, A.E., and Mootha, V.K. (2010). MICU1 encodes a mitochondrial EF hand protein required for Ca(2+) uptake. Nature *467*, 291-296.

Pfeiffer, T., Schuster, S., and Bonhoeffer, S. (2001). Cooperation and competition in the evolution of ATP-producing pathways. Science *292*, 504-507.

Pinton, P., Ferrari, D., Rapizzi, E., Di Virgilio, F., Pozzan, T., and Rizzuto, R. (2001). The Ca2+ concentration of the endoplasmic reticulum is a key determinant of ceramide-induced apoptosis: significance for the molecular mechanism of Bcl-2 action. EMBO J *20*, 2690-2701.

Porporato, P.E., Payen, V.L., Perez-Escuredo, J., De Saedeleer, C.J., Danhier, P., Copetti, T., Dhup, S., Tardy, M., Vazeille, T., Bouzin, C.*, et al.* (2014). A mitochondrial switch promotes tumor metastasis. Cell Rep *8*, 754-766.

Quintero, M., Brennan, P.A., Thomas, G.J., and Moncada, S. (2006). Nitric oxide is a factor in the stabilization of hypoxia-inducible factor-1alpha in cancer: role of free radical formation. Cancer Res *66*, 770-774.

Racker, E. (1976). Why do tumor cells have a high aerobic glycolysis? J Cell Physiol *89*, 697-700.

Raffaello, A., De Stefani, D., Sabbadin, D., Teardo, E., Merli, G., Picard, A., Checchetto, V., Moro, S., Szabo, I., and Rizzuto, R. (2013). The mitochondrial calcium uniporter is a multimer that can include a dominant-negative pore-forming subunit. EMBO J *32*, 2362-2376.

Rizzuto, R., De Stefani, D., Raffaello, A., and Mammucari, C. (2012). Mitochondria as sensors and regulators of calcium signalling. Nat Rev Mol Cell Biol *13*, 566-578.

Rizzuto, R., Pinton, P., Carrington, W., Fay, F.S., Fogarty, K.E., Lifshitz, L.M., Tuft, R.A., and Pozzan, T. (1998). Close contacts with the endoplasmic reticulum as determinants of mitochondrial Ca2+ responses. Science *280*, 1763-1766.

Rizzuto, R., Simpson, A.W., Brini, M., and Pozzan, T. (1992). Rapid changes of mitochondrial Ca2+ revealed by specifically targeted recombinant aequorin. Nature *358*, 325-327.

Rozen, S., and Skaletsky, H. (2000). Primer3 on the WWW for general users and for biologist programmers. Methods Mol Biol *132*, 365-386.

Sancak, Y., Markhard, A.L., Kitami, T., Kovacs-Bogdan, E., Kamer, K.J., Udeshi, N.D., Carr, S.A., Chaudhuri, D., Clapham, D.E., Li, A.A.*, et al.* (2013). EMRE is an essential component of the mitochondrial calcium uniporter complex. Science *342*, 1379-1382.

Santo-Domingo, J., Vay, L., Hernandez-Sanmiguel, E., Lobaton, C.D., Moreno, A., Montero, M., and Alvarez, J. (2007). The plasma membrane Na+/Ca2+ exchange inhibitor KB-R7943 is also a potent inhibitor of the mitochondrial Ca2+ uniporter. Br J Pharmacol *151*, 647-654.

Sarkar, S., Floto, R.A., Berger, Z., Imarisio, S., Cordenier, A., Pasco, M., Cook, L.J., and Rubinsztein, D.C. (2005). Lithium induces autophagy by inhibiting inositol monophosphatase. J Cell Biol *170*, 1101-1111.

Sciacovelli, M., Gaude, E., Hilvo, M., and Frezza, C. (2014). The metabolic alterations of cancer cells. Methods Enzymol *542*, 1-23.

Semenza, G.L. (2000). Hypoxia, clonal selection, and the role of HIF-1 in tumor progression. Crit Rev Biochem Mol Biol *35*, 71-103.

Semenza, G.L. (2002). Involvement of hypoxia-inducible factor 1 in human cancer. Intern Med *41*, 79-83.

Semenza, G.L. (2009). Regulation of oxygen homeostasis by hypoxia-inducible factor 1. Physiology (Bethesda) *24*, 97-106.

Semenza, G.L. (2010a). Defining the role of hypoxia-inducible factor 1 in cancer biology and therapeutics. Oncogene *29*, 625-634.

Semenza, G.L. (2010b). HIF-1: upstream and downstream of cancer metabolism. Curr Opin Genet Dev *20*, 51-56.

Sena, L.A., and Chandel, N.S. (2012). Physiological roles of mitochondrial reactive oxygen species. Mol Cell *48*, 158-167.

Shim, H., Dolde, C., Lewis, B.C., Wu, C.S., Dang, G., Jungmann, R.A., Dalla-Favera, R., and Dang, C.V. (1997). c-Myc transactivation of LDH-A: implications for tumor metabolism and growth. Proc Natl Acad Sci U S A *94*, 6658-6663.

Shimomura, O. (1986). Isolation and properties of various molecular forms of aequorin. Biochem J *234*, 271-277.

Taddei, M.L., Parri, M., Mello, T., Catalano, A., Levine, A.D., Raugei, G., Ramponi, G., and Chiarugi, P. (2007). Integrin-mediated cell adhesion and spreading engage different sources of reactive oxygen species. Antioxid Redox Signal *9*, 469-481.

Thannickal, V.J., and Fanburg, B.L. (2000). Reactive oxygen species in cell signaling. Am J Physiol Lung Cell Mol Physiol *279*, L1005-1028.

Tochhawng, L., Deng, S., Pervaiz, S., and Yap, C.T. (2013). Redox regulation of cancer cell migration and invasion. Mitochondrion *13*, 246-253.

Tomlinson, I.P., Alam, N.A., Rowan, A.J., Barclay, E., Jaeger, E.E., Kelsell, D., Leigh, I., Gorman, P., Lamlum, H., Rahman, S.*, et al.* (2002). Germline mutations in FH predispose to dominantly inherited uterine fibroids, skin leiomyomata and papillary renal cell cancer. Nat Genet *30*, 406-410.

Ursini, F., Maiorino, M., Brigelius-Flohe, R., Aumann, K.D., Roveri, A., Schomburg, D., and Flohe, L. (1995). Diversity of glutathione peroxidases. Methods Enzymol *252*, 38-53.

Vander Heiden, M.G., Cantley, L.C., and Thompson, C.B. (2009). Understanding the Warburg effect: the metabolic requirements of cell proliferation. Science *324*, 1029-1033.

Vander Heiden, M.G., Locasale, J.W., Swanson, K.D., Sharfi, H., Heffron, G.J., Amador-Noguez, D., Christofk, H.R., Wagner, G., Rabinowitz, J.D., Asara, J.M.*, et al.* (2010). Evidence for an alternative glycolytic pathway in rapidly proliferating cells. Science *329*, 1492-1499.

Vaupel, P., and Harrison, L. (2004). Tumor hypoxia: causative factors, compensatory mechanisms, and cellular response. Oncologist *9 Suppl 5*, 4-9.

Vaupel, P., and Mayer, A. (2007). Hypoxia in cancer: significance and impact on clinical outcome. Cancer Metastasis Rev *26*, 225-239.

Vaupel, P., Mayer, A., and Hockel, M. (2004). Tumor hypoxia and malignant progression. Methods Enzymol *381*, 335-354.

Wang, R., and Green, D.R. (2012). Metabolic checkpoints in activated T cells. Nat Immunol *13*, 907-915.

Wang, Y., Zang, Q.S., Liu, Z., Wu, Q., Maass, D., Dulan, G., Shaul, P.W., Melito, L., Frantz, D.E., Kilgore, J.A.*, et al.* (2011). Regulation of VEGF-induced endothelial cell migration by mitochondrial reactive oxygen species. Am J Physiol Cell Physiol *301*, C695-704.

Warburg, O. (1956). On the origin of cancer cells. Science *123*, 309-314.

Warburg, O., Wind, F., and Negelein, E. (1927). The Metabolism of Tumors in the Body. J Gen Physiol *8*, 519-530.

Weinhouse, S. (1976). The Warburg hypothesis fifty years later. Z Krebsforsch Klin Onkol Cancer Res Clin Oncol *87*, 115-126.

Weisiger, R.A., and Fridovich, I. (1973). Superoxide dismutase. Organelle specificity. J Biol Chem *248*, 3582-3592.

Wu, W.S. (2006). The signaling mechanism of ROS in tumor progression. Cancer Metastasis Rev *25*, 695-705.

Wu, W.S., Tsai, R.K., Chang, C.H., Wang, S., Wu, J.R., and Chang, Y.X. (2006). Reactive oxygen species mediated sustained activation of protein kinase C alpha and extracellular signal-regulated kinase for migration of human hepatoma cell Hepg2. Mol Cancer Res *4*, 747-758.

Zhang, J., Nuebel, E., Daley, G.Q., Koehler, C.M., and Teitell, M.A. (2012). Metabolic regulation in pluripotent stem cells during reprogramming and self-renewal. Cell Stem Cell *11*, 589-595.